UNIVERSITY OF CALIFORNIA, SAN DIEGO

Characterization of the Mechanism of Action of Transportin in Mitotic Spindle Assembly

A Thesis submitted in partial satisfaction of the requirements for the degree of Master of Science

in

Biology

by

Mary Elizabeth Swift-Taylor

Committee in charge:

Professor Douglass J. Forbes, Chair
Professor Maho Niwa Rosen
Professor James Wilhelm

2011

The Thesis of Mary Elizabeth Swift-Taylor is approved, and it is acceptable in quality and form for publication on microfilm and electronically:

Chair

University of California, San Diego

2011

TABLE OF CONTENTS

LIST OF ABBREVIATIONS

Nuclear Pore Complex (NPC)

Nuclear Localization Sequence (NLS)

Nucleoporin (Nup)

Maltose Binding Protein (MBP)

Glutathione s-Transferase (GST)

Truncated loop karyopherin β2 (TLB)

Transportin (Trn)

Guanine Exchange Factor (GEF)

Guanine Triphosphate (GTP)

GTPase Activating Protein (GAP)

Proline-Tyrosine (PY)

Phenylalanine-Glycine (FG)

Spindle Assembly Factor (SAF)

Cytostatic Factor (CSF)

Huntingtin, Elongation factor 3, regulatory subunit A, TOR1 (HEAT)

Hydrophobic proline-tyrosine nuclear localization sequence (hPY-NLS)

Basic proline-tyrosine nuclear localization sequence (bPY-NLS)

LIST OF FIGURES

ACKNOWLEDGEMENTS

I would like to acknowledge Professor Douglass J. Forbes for her support as the chair of my committee and the Principle Investigator of the lab. Her support and leadership has taught me more about the scientific world than I thought possible.

I would like to acknowledge Dr. Cyril Bernis, my mentor in this project. His guidance and patience made it possible for me to learn and proficiently use an entire new skill set.

I would also like to acknowledge the other members of the Forbes lab – Michelle Gaylord, Dr. Boris Fichtman, Steve Martell, and Sal Luna - without whom I would not have had the support to complete this project.

I would like to thank Dr. Yuh Min Chook of University of Texas, Southwestern for her generous donation of the molecules M9M and TLB.

Chapter 1 is currently being prepared for submission for publication. Bernis, Cyril; Swift-Taylor, Mary Elizabeth; Forbes, Douglass J. "Characterization of the Mechanism of Action of Transportin in Mitotic Spindle Assembly." I am a co-author in this publication.

ABSTRACT OF THE THESIS

Characterization of the Mechanism of Action of Transportin in Mitotic Spindle Assembly

by

Mary Elizabeth Swift-Taylor

Master of Science in Biology

University of California, San Diego, 2011

Professor Douglass J. Forbes, Chair

In eukaryotic cells, proteins known as karyopherins function during interphase as nuclear import and export receptors. Importin β and Transportin, two such karyopherins, act to carry proteins with different recognition sites into the interphase nucleus. Once inside the nucleus, these karyopherins exchange their cargoes for RanGTP, which is exclusively nucleoplasmic. Interestingly, Importin β has a very different role in mitosis. There it acts as a spatial regulator of mitotic events, including spindle assembly. Importin β masks spindle assembly factors everywhere except in the vicinity of chromatin, where a high concentration of RanGTP exists. Recently, our lab demonstrated that Transportin also regulates mitotic events. However, the mechanism for this was not explored.

Firm in the knowledge of Importin β's regulation of mitotic events, there are two obvious models for Transportin's regulation of spindle assembly. One is that Transportin acts by binding to and titrating RanGTP, thus modulating the release of spindle assembly factors by Importin β. A second is that, like Importin β, Transportin functions directly in spindle assembly, itself binding and masking a set of spindle assembly factors.

We employed different tools to test these mechanisms: M9M, a known inhibitor of Transportin in nuclear import, and TLB, a Transportin mutant with a truncated H8 loop that is desensitized to Ran-mediated cargo release. We used these molecular tools both in an *in vitro* extract derived from *Xenopus laevis* eggs and in an *in vivo* system, HeLa cells. Our results support the hypothesis that Transportin acts during mitosis, not indirectly through the titration of RanGTP, but directly by regulating spindle assembly factors. Potential factors will be discussed.

Introduction

In eukaryotes, the genomic DNA is enclosed and protected by the nuclear envelope. During interphase this envelope separates the cell into two distinct domains: one for replication and transcription and another for translation. However, molecules such as transcription factors, DNA replication and repair proteins, and messenger RNAs, of necessity, have to transport through the nuclear envelope. In order for this to occur, they must pass through an elaborate macromolecular gateway, the nuclear pore complex (NPC) (Allen *et al.*, 2000). The nuclear pore complex is a massive 120MD structure that perforates the nuclear envelope and is comprised of approximately 30 different nucleoporins (Nups) (Reichelt *et al.*, 1990; Lim *et al*, 2008; Rout *et al.*, 2000; Cronshaw *et al.*, 2002).

In interphase, the nuclear pore complex acts as a passage for molecules entering or exiting the nucleus (Hinshaw *et al.*, 1992). Macromolecules and proteins smaller than 20-40kD can move passively through the nuclear pore complex in an unassisted manner (Paine *et al.*, 1975). However, transport of proteins, RNAs, or viruses greater than 40 kD require active transport through the pore (Feldherr *et al.*, 1984). This transport process is in large part governed by two sets of players: the small GTPase Ran and a family of transport receptor proteins known as karyopherins (Chook and Suel, 2010).

The Basics of Nuclear Transport: Ran and Karyopherins

Ran is a small, 40 kD GTPase, related to Ras (Ren *et al.*, 1993). Ran exists in its GTP-bound state primarily in the nucleus. This is due to the fact that the guanine

exchange factor, or GEF, for Ran, RCC1, is a chromatin-bound protein (Bischoff *et al.*, 1991). In contrast, RanGAP1, the GTPase activating protein for Ran, is not found in the nucleus but is found bound to the cytoplasmic side of the nuclear pore complex as well as soluble in the cytoplasm (Bischoff *et al.*, 1994). The asymmetry of RanGEF and RanGAP creates an asymmetric gradient of Ran between the nucleoplasm (RanGTP) and cytoplasm (RanGDP). In order to replenish the supply of RanGTP within the nucleus, RanGDP is constantly shuttled into the nucleus by NTF2 (nuclear transport factor 2), whereupon RCC1 exchanges the GDP for GTP (Smith *et al.*, 1998). Figure 1 shows a depiction of the Ran cycle in interphase.

The karyopherin family of transport receptors contains members vital to both nuclear import and nuclear export (Marelli *et al.*, 2001). Known collectively as karyopherin-β proteins, they make use of the Ran gradient to transport cargo into or out of the nucleus (Chook *et al.*, 2001). Generally, karyopherins are large proteins of 90-130kD, with low sequence homology outside of a common N-terminal RanGTP-binding domain (Mosammaparast and Pemberton, 2004). All are composed of HEAT repeats (Chook and Suel, 2010).

The karyopherins specific for nuclear import, known as importins, bind receptor-specific cargo in the cytoplasm. They do so by recognition of a specific nuclear localization sequence or domain (Xu *et al.*, 2010). The karyopherin:cargo import complex then moves into the nucleus via interaction with the phenylalanine-glycine (FG) repeats found on a number of the nuclear pore proteins (Bayliss *et al.*, 2000; Frey *et al*, 2006). Once inside the nucleus, an import receptor releases its cargo upon binding

RanGTP and import is complete (Rexach and Blobel, 1995). The process of karyopherin-mediated nuclear import is depicted in Figure 2.

Export karyopherins, also known as exportins, are quite different in action. An exportin forms a trimeric complex within the nucleus. This trimeric complex consists of the export receptor, a nuclear export signal (NES)-containing cargo, and RanGTP (Stade *et al.*, 1997; Cook and Conti, 2010). RanGTP stabilizes the export complex and is, in fact, an integral part of it. After translocation of the complex through the nuclear pore, the RanGTP subunit of the export complex encounters RanGAP1, which causes hydrolysis of RanGTP to RanGDP. The export complex then dissociates, releasing the export cargo and RanGDP to the cytoplasm.

Two Key Karyopherins: Importin β and Transportin

The two most well studied members of the karyopherin family are Importin β (karyopherin-β1) and Transportin (karyopherin-β2). Both serve as import receptors that recognize distinct cargoes in the cytoplasm and transport them into the nucleus through the nuclear pore complex.

Importin β, a 96 kD protein, was the first nuclear import receptor discovered (Gorlich *et al.*, 1994). Importin β often uses an adapter protein, Importin α (Gorlich *et al.*, 1995), to import cargoes which have a classic mono- or bipartite nuclear localization sequence (NLS) into the nucleus (Conti *et al.*, 1998). Importin β, however, can also vary in its adapters and cargos and has been extensively reviewed (Gorlich and Kutay, 1999; Harel and Forbes, 2004; Chook and Suel, 2010)

Transportin is a 90 kD transport receptor that functions without an adapter. The crystal structure of Transportin shows two perpendicular arches made of HEAT repeats (Chook and Blobel, 1999). HEAT repeats are stretches of 39 amino acid residues that form helices (Andrade and Bork, 1995; Groves *et al.*, 1999). Thus, Transportin is a largely helical structure, and can be divided into three segments of HEAT repeats: one near the N-terminus that contains the RanGTP-binding domain, and two, including the C-terminal end, that make up the cargo-binding domain (Cansizoglu and Chook, 2007).

Transportin was originally discovered as the import receptor for the mRNA export protein hnRNP A1 (Pollard *et al.*, 1996). HnRNP A1 does not contain a classical recognition sequence for Importin β, but rather a distinct NLS: a 38 amino acid sequence that is recognized exclusively by Transportin. This specific sequence was termed the M9-NLS and is found only in hnRNP A1 (Lee *et al.*, 2006). It has been further shown that a 19 amino acid stretch of the M9 sequence, deemed the 'M9 core', is sufficient for import (Iijima *et al.*, 2006). In general, however, the NLSs recognized by Transportin are variable (Lee *et al.*, 2006). Transportin can bind to a variety of sequences, collectively termed the PY-NLSs, that have a C-terminal consensus sequence R/H/K/$X_{(2-5)}$PY. Within these varied NLSs, classes have been defined based on shared residues. The hydrophobic class of Transportin cargoes, containing what is referred to as hPY-NLSs, has four hydrophobic residues preceding the PY sequence, while the basic class of Transportin cargoes, containing what is referred to as bPY-NLSs, has N-terminal basic amino acid residues but no hydrophobic residues (Lee *et al*., 2006). When loaded with a PY-NLS cargo, Transportin then binds specifically to Nup358 in the nuclear pore complex for its passage into the nucleus (Hutten *et al*., 2008).

Transportin: Roles in Disease

Transportin serves as the import receptor for many mRNA-binding export proteins. Often, it is the target of disease agents that aim to stop a cell's native protein production in various ways. In Human Papillomavirus type 11 and 16, the L1 major capsid protein inhibits Transportin-mediated nuclear import (Nelson *et al*., 2002). The capsid protein, which is imported into the nucleus by Importin β (Merle *et al*., 1999), works in the nucleus to package and export virions, which can subsequently infect other cells. By blocking import by Transportin, the amount of proteins related to mRNA processing and export decreases within the nucleus, freeing materials inside the nucleus for viral replication.

Transportin also serves as the import receptor for HIV-1 (human immunodeficiency virus type-1) Rev protein, the protein required for the nuclear export of unspliced HIV viral RNA as well as for the nuclear import of HIV viral integrase (Hutten *et al*., 2008; Pollard *et al*., 1998; Levin *et al*., 2010). Interestingly, it has been found that blocking the Transportin-mediated import of the viral integrase protein drastically lowers the efficiency of HIV infection of a cell.

Transportin is also the import receptor for the protein FUS (fused in sarcoma). When the C-terminal PY-NLS of *fus* is mutated, it causes an unusual cytoplasmic accumulation of *fus*, as Transportin can no longer import *fus* into the nucleus. This inherited mutation is one cause of familial amyotrophic lateral sclerosis (fALS) (Dormann *et al*., 2010).

Lastly, Transportin has been shown to be the import receptor for DNA, both in transfection and in *in vitro* DNA import (Lachish-Zalait *et al.*, 2009). Thus, Transportin may well be important to mechanisms of gene therapy.

Karyopherins in Mitosis

The karyopherin Importin β has an interesting and entirely different role in mitosis. To be specific, Importin β has been shown to negatively regulate spindle assembly, nuclear membrane assembly, and nuclear pore assembly (Nachury *et al*., 2001). Clearly, formation of a spindle is desirous only around chromosomes. Due to the presence of the RanGEF, RCC1, exclusively on chromatin, a RanGTP "cloud" exists only in the vicinity of chromatin (Kaleb and Heald, 2008; Clarke and Zhang, 2008). It has been shown that Importin β has been co-opted by evolution to act as a critical negative regulator for spindle assembly. In essence, Importin β binds and masks spindle assembly factors (SAFs); it does so everywhere except in the vicinity of chromatin. Figure 3 shows a depiction of the mechanism by which Importin β acts to negatively regulate spindle assembly: near chromatin, RanGTP is produced. It binds to adjacent Importin β:SAF complexes, freeing the SAFs for action. In this manner, spindles form around the mitotic chromosomes and not elsewhere within the mitotic cell.

Interestingly, during interphase it has been noted that Importin β imports these same spindle assembly factors into the nucleus, likely to prevent them from interfering with interphase microtubule network structure (Harel and Forbes, 2004).

Among the spindle assembly factors that Importin β has been shown to regulate are the Nuclear Mitotic Apparatus protein (NuMA) (Nachury *et al.*, 2001), the

microtubule binding protein TPX2 (Gruss *et al.*, 2001), and lamin B. Lamin B, for example, serves in mitosis as part of the matrix that acts to organize other spindle assembly factors to form the spindle (Tsai *et al.*, 2006). A more comprehensive list will be presented in the Discussion.

Recently, Transportin was found by our laboratory to also have negative regulatory effects on spindle assembly, nuclear membrane assembly, and nuclear pore assembly in mitosis (Lau *et al.*, 2009). However, the overarching mechanism by which Transportin mediates this negative regulation was unknown. Two distinct types of mechanisms for this process can be postulated. In the first, Transportin could serve as a modulator for Importin β by titrating up RanGTP. Transportin, by binding and decreasing the concentration of available RanGTP, could thereby modulate Importin β's ability to release spindle assembly factors in the vicinity of chromatin, thus controlling the size or extent of the spindle (Ran Titration Model, Figure 4A). Alternatively, Transportin could have a more direct role in spindle assembly by directly regulating spindle assembly factors. In this model, Transportin would regulate SAF activity by binding and masking SAFs everywhere except in the vicinity of chromatin, where RanGTP is produced (Direct Inhibition Model, Figure 4B). Transportin could bind either a unique or overlapping set of SAFs to those regulated by Importin β. Thus, the focus of this thesis was to characterize the mechanism by which Transportin negatively regulates spindle assembly.

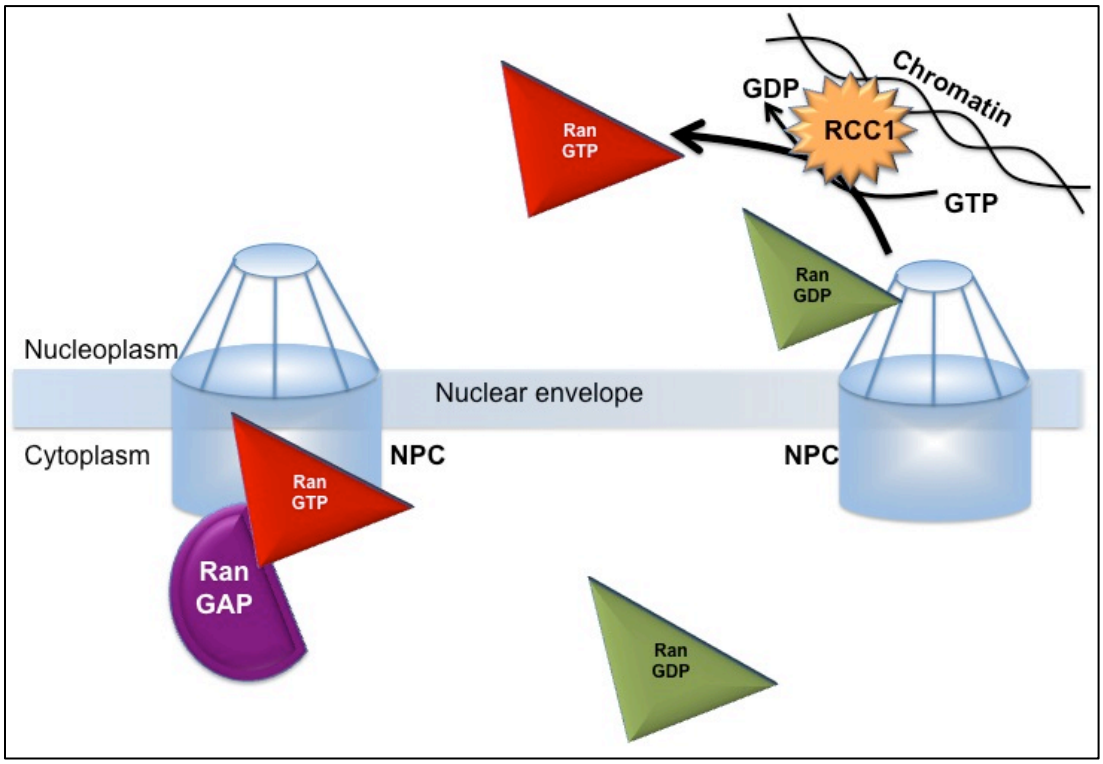

Figure 1 – The Ran Cycle
When RanGDP enters the nucleus, it encounters its guanine exchange factor (GEF), chromatin-bound RCC1, which exchanges the GDP for GTP. As RanGTP exits the nucleus through the nuclear pore complex, it encounters its GTPase activating protein, RanGAP. RanGAP is either soluble in the cytoplasm or bound to the cytoplasmic filaments of the nuclear pore (shown here). RanGAP causes RanGTP to hydrolyze its GTP, forming RanGDP. It should be noted that Ran's migration into and out of the nucleus is not random; rather, RanGTP moves into the nucleus aided by a specific import facilitator, NTF2, and exits the nucleus as a part of karyopherin export complexes.

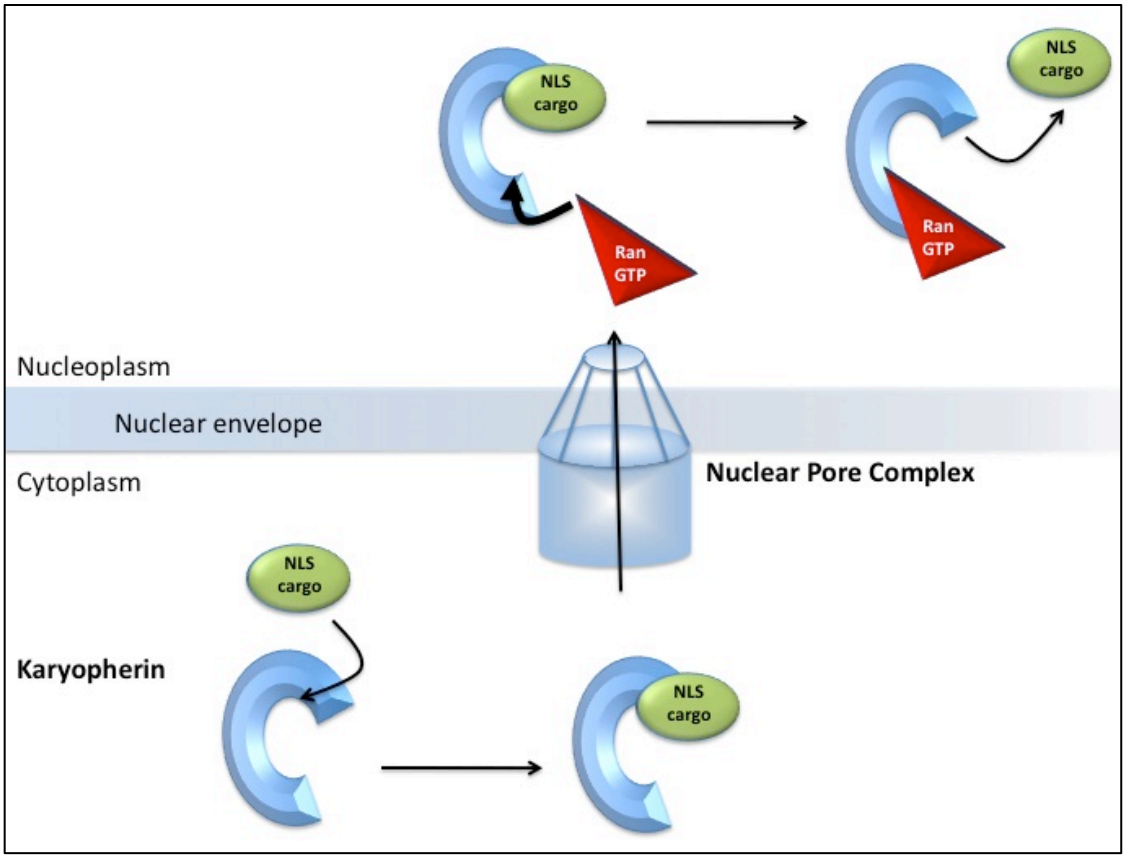

Figure 2 – General Mechanism of Nuclear Import
In the cytoplasm, a nuclear import receptor, known as an import karyopherin, binds to a specific cargo via a nuclear localization sequence (NLS) located within the cargo. This import complex then moves into the nucleus by interacting with the FG repeats on a subset of nucleoporins in the nuclear pore complex (NPC). Once inside the nucleus, the receptor binds RanGTP, which causes the receptor to change conformation and release the cargo, completing import.

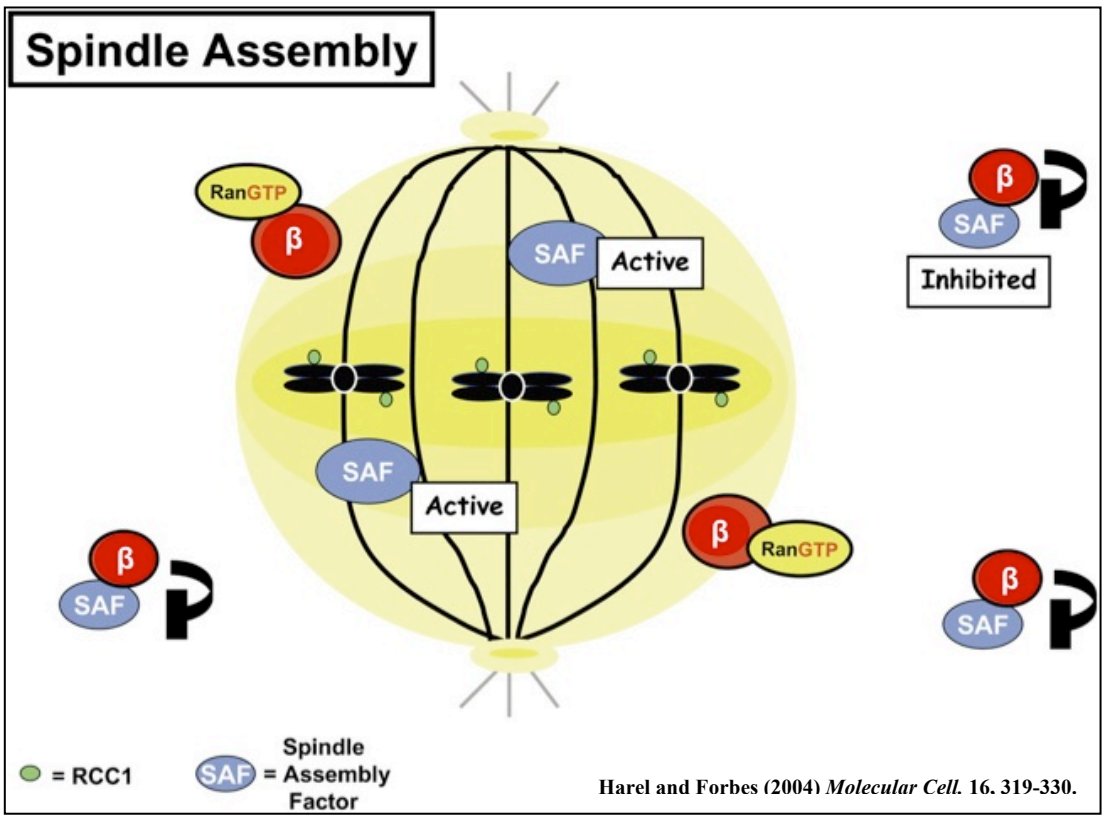

Figure 3 – Regulation of Spindle Assembly by Importin β
During mitosis, spindle assembly is negatively regulated by Importin β. Importin β binds and masks spindle assembly factors (SAFs) globally except in the vicinity of chromatin, where there exists a high concentration of RanGTP (yellow). When SAF-laden Importin β encounters RanGTP, Importin β releases the SAF upon binding RanGTP. This causes an accumulation of active spindle assembly factors specifically in the vicinity of the condensed chromosomes, thus restricting spindle assembly to this specific location.

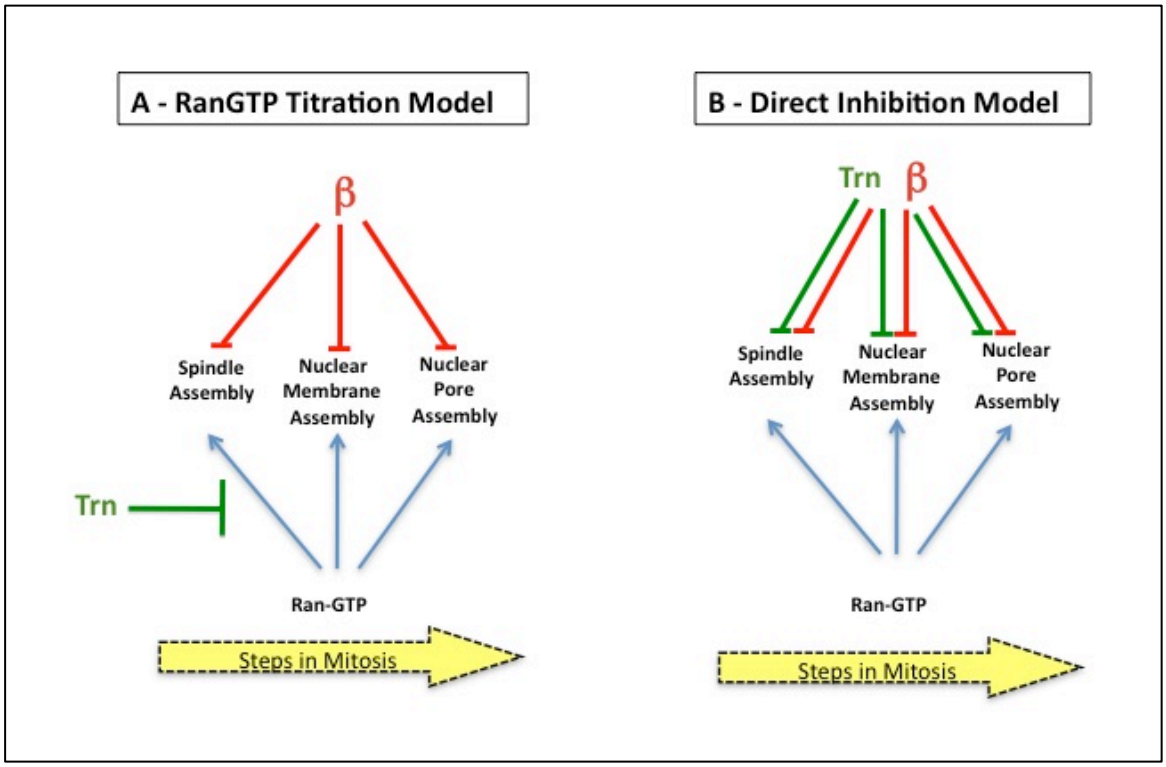

Figure 4 – Two Classes of Models for Transportin's Regulation of Mitotic Events
Two distinct models for Transportin's regulation of mitosis are shown. (**A**) Transportin acts as an indirect regulator of Importin β by modulating RanGTP. Due to Importin β's dependence on RanGTP to release spindle assembly factors (SAFs), this would indirectly regulate Importin β's regulation of mitotic events. (**B**) Transportin plays a direct role in spindle assembly, much like Importin β, regulating SAFs by binding and masking them everywhere except in the vicinity of the RanGTP cloud around chromatin.

Materials and Methods

Antibodies

Antibodies used for immunoblotting were mouse anti-human Transportin (BD Biosciences, San Jose, CA) and anti-Xenopus Importin β (Delmar *et al*., 2008). For immunofluorescence on HeLa cells, antibodies included a TRITC-labeled anti-myc antibody (Santa Cruz Biotechnology, Santa Cruz, CA), and a FITC-labeled anti-tubulin antibody (DM1A clone, SigmaAldrich, St. Louis, MO).

Recombinant Proteins

GST- human Transportin, GST-RanQ69L, and the recombinant form of the Transportin mutant TLB (Chook *et al*., 2002), GST-TLB, were expressed in Rosetta *E. coli* cells from pGEX6P vectors (Lau *et al.*, 2009; Harel *et al*., 2003; a gift from Yuh Min Chook). One liter LB-ampicillin cultures were grown at 37^{o}C until OD = 0.3-0.6 and induced for 4 hours with 1 mM IPTG.

GST- *Xenopus* Importin β was expressed in Rosetta *E. coli* cells from pGEX6P vectors (Delmar *et al*., 2008). One liter LB-ampicillin cultures were grown at 37^{o}C until OD = 0.3, then moved to a 16^{o}C water bath. The cultures were then induced with 0.3 mM IPTG for 4 hours, and after with 0.7 mM IPTG overnight (~12 hours).

All GST-tagged proteins were purified on Glutathione Sepharose beads (BioWorld, Dublin, OH) according to manufacturer's specifications and were eluted from the beads using a Glutathione solution (50 mM, pH 7.5).

The GST tag was removed from Transportin (when indicated) and from RanQ69L by proteolytic digestion using GSTPreScission Protease (GE Healthcare, Piscataway, NJ)

overnight at 4^0C according to the manufacturer's protocol, as described in Lau *et al*. (2009).

RanQ69L was loaded with GTP as described here. The protein was dialyzed into 1X PBS (127 mM NaCl, 2.7 mM KCl, 1.5 mM KH_2PO_4, 32 mM Na_2HPO_4) and concentrated to a final volume of 950 µL. A 50 µL reaction buffer containing GTP (30 µL GTP, 20 µL 0.5 M EDTA, 1 µL 1 M DTT) was added and the mixture was incubated for 1 hour at room temperature. The reaction was stopped by incubating on ice for 15 minutes, followed by the addition of 31 µL of 1 M $MgCl_2$.

Maltose binding protein (MBP), MBP-M9, and MBP-M9M were expressed in Rosetta *E. coli* cells from pMAL vectors that were a kind gift from Yuh Min Chook (Cansizoglu *et al*., 2007). One liter LB-ampicillin cultures were grown at 37^oC until OD = 0.3-0.6 and induced for 4 hours with 1 mM IPTG. All MBP-tagged proteins were purified on Amylose Resin (NE Biolabs, Beverly, MA) according to manufacturer's specifications and eluted with Maltose Elution Buffer (Tris 50 mM, NaCl 50 mM, Maltose 50 mM, pH 7.5).

All proteins were dialyzed into XB (Xenopus buffer: 50 mM Sucrose, 10 mM HEPES, 100 mM KCl, 1 mM $MgCl_2$, 0.1 mM $CaCl_2$) and stored in 5 µL aliquots at -80^oC.

Xenopus Egg Extract

A mitotic *Xenopus* egg extract was used as an *in vitro* system for studying spindle assembly. The protocol used to make different extracts is given below and in Lau *et al*. (2009).

To obtain *Xenopus laevis* eggs, the frogs were primed for ovulation by injection of 100 U Pregant Mare Serum Gonadotropin (Balbiochem, La Jolla, CA), followed by rest in a bucket with 100 mM NaCl and 0.1 mM $Na_2S_2O_3$ overnight at 18^oC. The frogs were then induced to ovulate by injection of 500 U human chorionic gonadotropin (Sigma-Aldrich, St. Louis, MO) and placement in separate buckets of 100 mM NaCl and 0.1 mM $Na_2S_2O_3$. They were allowed to lay eggs overnight. The eggs were collected the following morning.

Any dead or activated eggs were removed and the remaining eggs were washed with a cysteine solution (2%, pH 7.7) to remove the jelly surrounding them. To remove the cysteine, the eggs were washed with XB buffer (50 mM Sucrose, 10 mM HEPES, 100 mM KCl, 1 mM $MgCl_2$, 0.1 mM $CaCl_2$), for interphase extract, or XB-EGTA (XB supplemented with 7 mM EGTA), for mitotic (or CSF – cytostatic factor) extract. The eggs were then crushed by centrifugation for 15 minutes at 18,000 RCF in a TX-160 high-speed centrifuge (Tomy, Japan) using a TMH-21 rotor. The center cytoplasmic layer was drawn out using an 18-guage needle attached to a syringe. This was supplemented with cytochalasin B (50 μg/mL), aprotinin (10 μg/mL), and leupeptin (10 μg/mL) and centrifuged again for 15 minutes at 18,000 RCF. The middle layer after this spin is the extract, containing both the soluble fraction and membranes, and was recovered with a fresh 18-guage needle. The freshly prepared extracts were used directly in assembly experiments (as described below). Remaining extracts were frozen at -80^oC in 200 μL aliquots and were used in immunoblotting and protein experiments.

Quantification of Endogenous Transportin and Importin β in *Xenopus* Egg Extract

For Importin β quantification, 1 μL and 0.5 μL of interphase *Xenopus* extract were run on a PAGE-SDS gel against a set of recombinant GST-Importin β standards; the resulting gel was analyzed by immunoblotting with anti-Xenopus Importin β antibody. This experiment was repeated three times and the resulting bands on the autoradiographic film (Denville Scientific, Metuchen, NJ) were analyzed using ImageJ software according to the instructions found at http://rsbweb.nih.gov/ij/.

For Transportin quantification, 3 μL, 2 μL, and 1 μL of interphase *Xenopus* extract were run on a PAGE-SDS gel against a set of recombinant human Tranportin standards; the resulting gel was analyzed by immunoblotting. Xenopus and human Transportin show 99% identity, as determined by BLAST analysis, and as such an anti-human Transportin antibody will sufficiently recognize *Xenopus* Transportin (Lau *et al*., 2009). The experiment was repeated three times and the resulting bands on the autoradiographic film (Denville Scientific, Metuchen, NJ) were analyzed using ImageJ software according to the instructions found at http://rsbweb.nih.gov/ij/.

Xenopus Spindle Assembly Assay

To observe spindle assembly, we first added chromatin to *Xenopus* egg interphase extract, waited 1 hour for nuclei to form and the chromatin to replicate, and then induced mitosis. Specifically, interphase extract was incubated with Energy Mix (10 mM phosphocreatine, 80 μg/mL creatine kinase, 1 mM ATP, 2 mM $MgCl_2$, and 100 mM EGTA) and sperm chromatin (70,000 SpC per 20 μL extract) at room temperature for 2 hours to allow DNA replication. To induce mitosis, 10 μL of this reaction, which now

contains nuclei, was then mixed with 15 μL CSF extract, 1 μL rhodamine-labeled tubulin (Cytoskeleton, Denver, CO), and 2 μL of Energy Mix. Upon verification of mitotic conversion after 5 minutes, where noted, the following proteins were added: 20 μM GST, 10 μM RanQ69L-GTP, 20 μM GST-Transportin, 20 μM GST-TLB, 10 μM MBP, 10 μM MBP-M9, or 10 μM MBP-M9M. The reaction was incubated in the dark at room temperature. At 60 and 90 minutes, 2.5 μL were removed and mounted with 1 μL of fixation buffer (48% glycerol, 11% formaldehyde, 10 mM HEPES, 5 μg/mL Hoeschst, pH 7.5) on glass slides (Gold Seal, Portsmouth, NH). Slides were analyzed using a Zeiss Axioskop 2 microscope using a 63x objective. Between 50 and 100 microtubule structures or condensed chromatin packages were observed for each condition.

To measure spindle size, the surface area of approximately 20 spindles from the conditions MBP, MBP-M9M, and RanQ69L-GTP was measured using ImageJ software according to the instructions found at http://rsbweb.nih.gov/ij/.

MBP Pulldowns – Direct Interaction

To verify the interactions between recombinant proteins, direct interaction assays were performed. Recombinant MBP, MBP-M9, and MBP-M9M (130 μg each condition) were incubated with Amylose Resin (NE Biolabs, Beverly, MA) in Tris (50 mM, pH 7.5) for 30 minutes at room temperature, blocked with 2 mg Bovine Serum Albumin (BSA) for 30 minutes, and then washed 4 times with 1X PBS to remove any unbound proteins. The beads were then incubated with 100 μg each of GST-Transportin, GST-TLB, or GST for 1 hour at room temperature. After washing with NP40 lysis buffer (150 mM NaCl, 50 mM Tris-HCl, pH 7.5, 20 mM NaF, 5 mM EDTA, 1.75 mM β-glycerophosphate, 1 mM

sodium pyrophosphate, 1 mM PMSF, 1 mM sodium orthovanadate, 1% NP-40, 5 μg/mL aprotinin, 2 μg/mL pepstatin A, 2 μg/mL leupeptin) and Tris (50 mM, pH 7.5), bound proteins were eluted with 2X Sample Buffer (125 mM Tris, 20% glycerol, 4% SDS, 10% β-mercapethanol, 10 μM Bromophenol Blue, pH 6.8). The samples were loaded on an SDS-PAGE gel. The gel was then fixed (50% EtOH, 7% NaOAc) for 1 hour and stained with a 1:4 dilution of a solution of Coomassie Blue G250 (10% ammoniun sulfate, 2% phosphoric acid, 5% Coomassie Brilliant Blue G-250; ThermoScientific, Rockford, IL) and destained with water.

MBP Pulldowns – Endogenous Interaction

To verify the interactions between recombinant MBP constructs and endogenous Transportin, interaction assays were performed with immobilized MBP constructs and either mitotic or interphase *Xenopus* egg extracts. Recombinant MBP, MBP-M9, and MBP-M9M were incubated with Amylose Resin (NE Biolabs, Beverly, MA) in XB-EGTA (XB supplemented with 7 mM EGTA) for 30 minutes at room temperature, then blocked with 2 mg Bovine Serum Albumin (BSA) for 30 minutes. Beads were washed with XB-EGTA and incubated with *Xenopus* egg extract for 1 hour at room temperature. Pulldown reactions were washed with NP40 lysis buffer and then Tris (50 mM, pH 7.5). Bound proteins were eluted with 2X Sample Buffer. The samples were analyzed by immunoblotting.

In Vivo HeLa Cell Experiments

To observe and assess mitotic spindle assembly *in vivo*, HeLa cells were used. In 6-well plates, cover slips (12 mm) were placed in each well. 200,000 HeLa cells per well were seeded and grown overnight in a 37^0C incubator. Cells were then transfected using JetPI according to manufacturer's protocol (PolyPlus Transfection, France) with 2μg each of the mammalian expression vectors pCS2+MT MBP (control) or pCS2+MT MBP-M9M (a gift from Yuh Min Chook, TX; Cansizoglu *et al*., 2007). Cells were incubated at 37^oC for 24 hours.

Cells were fixed to coverslips with cold 100% methanol for 20 minutes and rehydrated with 1X PBS for 1 hour. The coverslips were prepared for standard immunofluorescence with TRITC-labeled anti-myc and FITC-labeled anti-tubulin antibodies (as described in Antibodies). Coverslips were mounted on slides with 2 μL Vectashield with DAPI mounting media (Vector Labs, Southfield, MI) and visualized with a Zeiss Axioskop 2 microscope using a 63x objective. Approximately 200 cells from each condition (MBP or MBP-M9M) were observed and the structures noted.

Chapter 1

Characterization of the Mechanism of Action of Transportin in Mitotic Spindle Assembly

Introduction

The focus of this thesis was to investigate the mechanism by which Transportin negatively regulates spindle assembly. Firm in the knowledge of the mechanism of Importin β's regulation of spindle assembly, there are two obvious mechanisms for Transportin's regulation of spindle assembly: Transportin serves as an indirect regulator for Importin β by modulating RanGTP (Ran Titration Model), or Transportin directly regulates spindle assembly by binding and masking spindle assembly factors (SAFs) everywhere except in the vicinity of chromatin (Direct Inhibition Model). To test these models, we used an *in vivo* system of HeLa cells and the powerful *in vitro* system of Xenopus egg extracts.

Xenopus laevis *egg extracts – An* in vitro *system for monitoring spindle assembly*

Cytosolic extracts derived from *Xenopus laevis* eggs provide a very convenient way to test these models. Such a system can be considered a cell-free micro-bioreactor in which we are able to reconstitute, *in vitro*, biochemical reactions and the assembly of structures identical those *in vivo*. Moreover, it only takes one hour to observe not only normal assembly, but also the effects that result from the addition of a recombinant protein or potential inhibitor. Therefore, cell-cycle specific *Xenopus laevis* egg extracts are a powerful tool for dissecting specific mechanisms and structures.

Upon ovulation, *Xenopus laevis* lay eggs naturally are arrested in the second metaphase of meiosis by Cytostatic Factor (or CSF). This stage is biochemically and physiologically related to a mitotic state. The observed arrest is the result of a set of

signaling pathways converging to stop the progression of the cell cycle. Normally, upon fertilization, a burst of calcium ions are released, ending the meiotic arrest and allowing the egg to move into interphase. To obtain an egg extract in mitotic arrest, the addition of the calcium chelator, EGTA, to the egg lysis buffer is fundamental. EGTA traps calcium ions when the eggs are lysed by centrifugation. The cytosol thus obtained has all the biochemical characteristics of intact mitotic eggs. The addition of 1μM $CaCl_2$ to mitotic extracts releases them into an interphase state by mimicking the calcium burst that occurs during fertilization (Chan and Forbes, 2006; Maresca and Heald, 2006). In this way, we can easily create extracts that are considered either interphase extracts or mitotic (CSF) extracts (for specific details, see Materials and Methods).

Within these extracts, we are able to assemble, *in vitro,* nuclei in interphase extracts or mitotic structures in mitotic extracts (Forbes *et al.*, 1983; Desai *et al.*, 1999). The addition of *Xenopus* sperm chromatin (as a source of DNA) and membranes to interphase egg extract cytosol produces nuclei. In contrast, addition of sperm chromatin to mitotic extracts produces mitotic spindles around condensed chromatin. The structures assembled *in vitro* are closely related to the structures observed in *in vivo* systems. The structures can be observed via fluorescence microscopy, after fixing a sample of the extract and mounting it between a glass slide and cover slip. Microtubule structures can be visualized by the addition of rhodamine-labeled tubulin to a mitotic extract, which integrates into microtubule structures alongside wild-type tubulin, while DNA becomes visible after Hoescht DNA dye staining.

Finally, we can also add recombinant proteins or drugs to the *Xenopus* egg extracts and observe how they affect the assembly of various structures. For example,

addition of recombinant proteins, antibodies, drugs, or ions can affect the assembly of structures and the biochemical reactions that occur.

Although the *Xenopus* system is a powerful *in vitro* tool to dissect major mechanisms, the study of these processes in an *in vivo* system, such as in HeLa cells, is also of interest to our hypothesis. The HeLa cell line can be efficiently transfected with DNA constructs, which leads to expression of the protein or inhibitor in question. In this way, it is possible to ascertain whether there are any phenotypic changes on the mitotic microtubule network that result from modification of Transportin's ability to function normally.

In testing the hypotheses on Transportin's mechanism of action, we used two recombinant proteins: (1) a synthetic hybrid signal sequence peptide called M9M, which is known to be an inhibitor of nuclear import by Transportin, and (2) a mutant form of Transportin, referred to here as TLB. Both proteins allowed us to observe changes in spindle assembly that resulted from modifying the functions of endogenous Transportin. The next section describes the two major tools used for this study.

M9M, a Synthetic Peptide Signal Sequence that Binds Transportin as Cargo

As previously described, Transportin recognizes and binds proteins that contain a PY (proline-tyrosine) nuclear localization sequence (NLS). Unlike the classical NLS recognized by Importin β, the PY-containing NLS can vary between different proteins. All PY-NLSs contain an R/K/Hx_{2-5}PY consensus sequence near the C-terminus of the NLS, but the upstream and downstream elements of the NLS sequence can be different. Because of this variation, classes of PY-NLSs have been defined based on shared

residues. The hydrophobic class of Transportin NLSs, referred to as hPY-NLSs, is characterized by four hydrophobic residues preceding the PY sequence. The basic class of Transportin NLSs, referred to as bPY-NLSs, has N-terminal basic amino acid residues but no hydrophobic residues (Lee *et al*., 2006). For example, the RNA binding protein hnRNP A1, which is imported by Transportin through the nuclear pore complex, contains a specific hPY-NLS, originally referred to as the "M9" NLS (Figure 5) (Siomi and Dreyfuss, 1995; Pollard *et al.*, 1996).

Interestingly, the two different classes of NLS recognized by Transportin have allowed for the creation of a potent inhibitor of Transportin, done by combining sections of the two PY-NLS into one synthetic peptide: M9M (Cansizoglu *et al*., 2007). M9M is a hybrid peptide, containing structural binding epitopes from each PY-NLS class. Specifically, M9M contains N-terminal elements from hnRNP A1, which contains an hPY-NLS, and C-terminal elements from hnRNP M, which contains a bPY-NLS (Figure 5). The combination of the two signal sequence causes M9M to have a three-dimensional structure that fits perfectly into the cargo-binding domain of Transportin. This results in tighter binding of M9M to Transportin and causes the Transportin-M9M complex to be greatly desensitized to Ran-mediated cargo release. M9M acts as a competitive inhibitor for Transportin, preventing Transportin from binding its endogenous cargoes and removing the native cargoes already bound to Transportin. In fact, the chimeric M9M peptide binds Transportin with a 200-fold tighter binding affinity than the M9 hPY-NLS of hnRNP A1 (Cansizoglu *et al*., 2007). Figure 5 shows the amino acid sequences for each of these peptides.

TLB, a Mutant Form of Transportin

The structure of Transportin is composed of two perpendicular arches. The N-terminal arch contains the RanGTP-binding domain, and the C-terminal arch contains the cargo-binding domain (Cansizoglu and Chook, 2007). Linking these two arches is a flexible acidic loop of amino acids, referred to as the H8 loop (Imasaki, 2007; Chook *et al*., 1999). Transportin recognizes and binds cargo containing a PY-NLS with its C-terminal arch. When the Transportin-cargo complex encounters RanGTP, Transportin binds the RanGTP within its N-terminal arch. This causes the H8 loop to bend and displace the cargo in the C-terminal arch (Figure 6) (Lee *et al*., 2006).

A mutant of Transportin had been constructed to have a deletion in the H8 loop; we refer to it as TLB for Truncated Loop karyopherin Beta2 (Chook *et al*., 2001). TLB can still bind cargoes and RanGTP, but because the H8 loop has been removed, the binding of RanGTP does not displace bound cargo. The deletion in TLB allows for binding of cargo and RanGTP simultaneously. Figure 6 depicts the mechanisms for wild-type Transportin and TLB's interaction with both cargo and RanGTP.

Here, we used *in vitro Xenopus laevis* egg extracts, as well as HeLa cells, and the recombinant proteins illustrated above to investigate the mechanism by which Transportin regulates spindle assembly.

Results

Concentration Determination of Endogenous Transportin

Above, two models for Transportin's regulation of mitotic events were described: (1) Transportin acts indirectly in mitotic events by regulating Importin β through the modulation of RanGTP, or (2) Transportin acts directly in mitotic events by binding and masking specific targets. A consideration in the evaluation of either model is the concentration of endogenous Transportin in the *Xenopus* egg extracts compared to the concentration of endogenous Importin β. As previously shown, Importin β exists in micromolar concentration in *Xenopus* egg extracts (Gorlich *et al*, 1993). However, the concentration of endogenous Transportin had not yet been determined.

Prior quantitation of endogenous Importin β in *Xenopus* egg extracts had been performed. However, at the time the authors assumed Importin β was 60 kD. Correcting for the current-day value of 96 kD, one estimates that Importin β is present at approximately 2.1 μM. Here, we repeated this quantitation experiment. First, GST-Importin β was produced and purified from *E. coli*. The recombinant protein was compared to the endogenous *Xenopus* Importin β present in egg extract via immunoblot analysis. Specifically, interphase *Xenopus* egg extract was compared to a set of increasing amounts of recombinant *Xenopus* GST-tagged Importin β (from 0.2 μg to 0.7 μg), as shown in Figure 7. The quantitation experiment was repeated three times. Using the analysis software ImageJ to quantify the immunoblot (see Materials and Methods), we determined that the concentration of endogenous Importin β present in *Xenopus* extract was on average at 6.5 μM (Figure 7).

Next, we performed the same quantitative immunoblot analysis for Transportin. GST-hTransportin was expressed and purified from *E. coli*, and the GST tag was then removed by proteolytic cleavage using Prescission Protease (see Materials and Methods). We were able to use an anti-human Transportin antibody because *Xenopus* and human Transportin have a 99% amino acid identity. By comparing the amount of Transportin present in *Xenopus* egg extract (1 μL, 2 μL and 3 μL of extract) to a set of recombinant Transportin standards (from 0.15 μg to 1.2 μg of recombinant Transportin), we determined the concentration of endogenous Transportin in *Xenopus* egg extract to average 7 μM (Figure 8). It should be noted that this experiment was performed three times and the average of the three experiments was taken. We conclude that endogenous Transportin and Importin β are comparable in concentration in *Xenopus* egg extracts.

However, the existence of comparable amounts of Transportin and Importin β would be consistent with either model of action of Transportin.

After determining the concentration of both Importin β and Transportin in *Xenopus* egg extracts, we next needed to verify that M9M could efficiently bind to Xenopus and recombinant Transportin. While the M9M peptide was made to contain a recognition sequence only for Transportin and not Importin β, these interactions had not yet been explored in *Xenopus* egg extract. Moreover, the M9M synthetic peptide has FG (Phenylalanine Glycine) residues, which are known to interact with Importin β, which could theoretically confer Importin β binding via a different mode. Since sequence analysis of M9M alone was not enough to exclude fully any potential interactions between M9M and Importin β, we had to verify experimentally that there was no such interaction. Nonspecific inhibition of Importin β by M9M would compromise any

Transportin data, so this interaction had to be ruled out. In addition, because we used GST- and MBP-tagged proteins in our experiments, it was also necessary to ensure that the tags were not interacting with one another or with the recombinant proteins.

First, we tested these interactions by performing direct interaction pull downs. For this, 130 μg of MBP, MBP-M9, or MBP-M9M were bound as bait to amylose resin. Then, 100 μg of recombinant GST-Transportin, GST-Importin β, or GST was added to each set of beads. After washing away the unbound proteins, the bound proteins were eluted and analyzed by PAGE-SDS gel electrophoresis and staining with G-250 Coomassie (Figure 9). Comparing the input samples of GST-Transportin, GST Importin β, and GST to the experimental pull downs, the only interaction observed was that of GST-Transportin and MBP-M9M (Figure 9, Lane 3). This was a critical finding because it meant that any results seen in subsequent experiments, following the addition of MBP-M9M, were due to the interaction between M9M and Transportin and not to an interaction between M9M and Importin β.

Importantly, neither GST alone nor MBP alone interacted with any constructs (Figure 9). This allows the conclusion that the interaction between GST-Transportin and MBP-M9M is due to Transportin interacting with M9M. It is also crucial that none of the MBP constructs interact with Importin β. With this data in mind, we can conclude that M9M interacts directly with Transportin and not with Importin β. This supports the idea that M9M is a direct binding and specific inhibitor of Transportin, confirming the work of Cansizoglu *et al* (2007).

However, while the direct interaction between Transportin and M9M was shown using recombinant proteins, the interactions between M9M and endogenous *Xenopus*

Transportin and Importin β had not been explored. As before, 130 μg of MBP, MBP-M9, or MBP-M9M were bound as bait to amylose resin. We then added 100 μL of either mitotic or interphase *Xenopus* egg extracts. After washing away unbound proteins, the bound proteins were eluted and run on PAGE-SDS. The results were analyzed by immunoblot (Figure 10).

In both types of extract, MBP was not able to pull down endogenous *Xenopus* Transportin or Importin-β (Figure 10, Lane 1). This indicates that MBP does not interact with either endogenous protein. MBP-M9 was able to pull down a very small amount of endogenous Transportin but no Importin β (Figure 10, Lane 2). In fact, this makes sense because M9 is an NLS for Transportin. Finally, MBP-M9M was able to pull down a significant amount of endogenous Transportin but no Importin β in either interphase or mitotic extracts (Figure 10; Lane 3). We conclude that, in both mitotic and interphase *Xenopus* egg extracts, M9M interacts strongly with Transportin but not Importin β.

These results show that using MBP-M9M could efficiently bind *Xenopus* Transportin. Previous experiments had shown such interaction in HeLa cells (Cansizoglu *et al*., 2007). The results here justify the use of MBP-M9M in our *Xenopus* experiments as a potent inhibitor of Transportin.

Transportin Inhibition in HeLa Cells Causes Defects in Mitosis and Cytokinesis

As shown above, M9M is an effective tool for binding Transportin in *Xenopus* egg extracts. M9M was also shown to bind Transportin and inhibit its nuclear import in HeLa cells (Cansizoglu *et al*., 2007). We set out to investigate the role of Transportin in mitotic events in HeLa cells through the use of the Transportin inhibitor M9M.

In order to observe M9M's effects *in vivo*, we transfected M9M into HeLa cells (Figures 11 and 12). HeLa cells were transfected overnight with myc-tagged MBP constructs (MBP or MBP-M9M) in pCS2+ myc-tagged vectors. Cells transfected with the myc-MBP constructs were visualized using a TRITC-labeled anti-myc antibody. Microtubule structures in the cells were visualized using a FITC-labeled anti-tubulin antibody, while DNA was visualized by DAPI. As controls, both cells transfected with MBP alone and non-transfected cells were observed.

We found that almost 30% of cells transfected with the Transportin inhibitor M9M showed defects in either mitosis or cytokinesis. Examples of structures found in such cells are shown in Figure 11; quantitation of the structures is shown in Figure 12. In the control conditions, approximately 3% of cells contained microtubule midbodies (Figure 12, "Midbodies"). A midbody containing microtubules is a normal structure observed in cells completing cytokinesis. In contrast, 18% of the M9M-transfected cells contained midbodies (Figure 11A). Furthermore, 13% of these M9M-transfected cells had both DNA bridges and microtubule midbodies, whereas no control cells had DNA bridges (Figure 11B). In addition to the above, another 6% of the M9M-transfected cells were multinucleate; less than 1% of control cells showed a multinucleate phenotype (Figure 11C). The observation of a multinucleate cell indicates that a cell had attempted to divide, failed, and the two daughter cells never were able to separate. These aberrant structures, i.e. increased midbodies, the presence of DNA bridges, and increased multinucleate cells, indicate that cells transfected with M9M had problems completing cytokinesis and were thus delayed in finishing this part of the cell cycle.

Another striking defect was seen in the mitotic spindles of M9M transfected cells.

In the control conditions (MBP or non-transfected cells), around 6% of cells showed a mitotic spindle. Approximately 5% of these cells containing mitotic spindles, or less than 1% of the total cells, showed any kind of abnormality (Figure 11E). Interestingly, for the M9M-transfected cells, while again 6% of the cells showed a mitotic spindle, 80% of these cells had defective spindles (Figure 11D). Instead of a normal bipolar spindle, these cells had chaotic, disorganized microtubule structures around the DNA. Thus, the abnormal spindles found in M9M transfected cells indicate that properly functioning Transportin is necessary for correct spindle assembly.

In sum, cells that were transfected with M9M showed clear defects in both mitosis and cytokinesis. These defects indicate that when M9M inhibited Transportin, the cells were unable to adequately complete mitosis. While this gives us a clear phenotype that correlates to Transportin-inhibited cells, it does not show the direct cause of this phenotype. Defects in cytokinesis could be due to the loss of Transportin's ability to directly regulate spindle assembly. However, Transportin also plays a significant role in nuclear import in interphase, so we cannot exclude the possibility that inhibiting Transportin stopped the import of potential spindle assembly factors or chromosomal proteins prior to mitosis; this could have caused microtubule organization issues later on in mitosis with multiple effects during cytokinesis.

Investigating Transportin's Regulation of Spindle Assembly in Xenopus Egg Extracts

Previous studies in our lab have shown that addition of Transportin to mitotic *Xenopus* egg extract inhibits spindle assembly (Lau *et al*., 2009). Taking into consideration that the inhibition of Transportin by M9M in HeLa cells caused striking

defects in mitosis and cytokinesis, we then addressed the question of the mechanism by which Transportin regulates spindle assembly in mitosis *in vitro*. We did this through the use of a system of spindle assembly in extract derived from *Xenopus laevis* eggs (Chan and Forbes, 2006; Maresca and Heald, 2006). We examined spindles and spindle assembly in this system specifically to address the question of whether Transportin functions in spindle assembly indirectly, by titrating RanGTP and modulating the function of Importin β, or directly, by binding and masking spindle assembly factors.

For this, we made both interphase and mitotic (CSF) extract from *Xenopus* eggs (see Materials and Methods). *Xenopus laevis* sperm chromatin was added to freshly prepared interphase extract supplemented with an ATP regenerating system. The system was incubated for one hour to allow for nuclei to form and chromatin to replicate. At this time, 15 μL of the reaction containing nuclei was added to 15 μL of freshly prepared CSF, i.e. mitotic, extract to induce mitosis. Rhodamine-labeled tubulin plus or minus recombinant proteins (see description of each condition below) were then added. After one hour at room temperature, 2 μL of each spindle assembly reaction was fixed on glass slides and visualized using fluorescence microscopy. Microtubules were visualized due to integration of the rhodamine-labeled tubulin, while chromatin was visualized by Hoescht DNA dye present in the fixation buffer.

We first analyzed the effects of adding MBP or MBP-M9M to the spindle assembly assay (Figure 13). When control MBP protein was added, the dominant structure, observed 77% of the time, was a normal bipolar spindle (Figure 13A). Also present were weak spindles (13%), half spindles (5%), and condensed chromatin lacking associated microtubules (4%).

We then examined spindle and microtubule structures in mitotic extracts to which MBP-M9M was added. One of the potential models for Transportin's regulation during mitosis is that Transportin binds spindle assembly factors (SAFs) to regulate spindle assembly. If that is the case, then what is the effect of M9M, a proposed competitive inhibitor of Transportin, on endogenous Transportin in mitotic *Xenopus* egg extract?

When MBP-M9M (10 μM) was added to a spindle assembly assay, 45% normal bipolar spindles were observed (Figure 13B). However, the remaining structures that formed differed from those observed in the MBP control. Very large spindles over a larger than normal amount of chromatin were observed as 15% of the structures. In addition, 26% of the total structures observed were asters, which are groups of spontaneous microtubule nucleation forming in the absence of chromatin. In addition, 8% of the observed structures were multipolar spindles (Figure 13B).

Surprisingly, the M9M results are reminiscent of the effect of adding excess RanGTP to mitotic *Xenopus* extract. RanQ69L is a constitutively active mutant form of the small GTPase Ran and is not able to hydrolyze GTP. To compare, we added excess RanQ69L-GTP (10 μM) itself to *Xenopus* extracts. With RanGTP, bipolar spindles were observed, but only 25% of the spindles would be considered normal – similarly bipolar shaped like the ones observed in the control condition - but these were significantly larger (Figure 13B). In addition, 8% of structures observed were also bipolar spindles, but they were also larger and now had more chromatin associated with them than control spindles. The dominant structures (48%) seen with RanGTP were large microtubule aster groups that formed in the absence of chromatin. Lastly, 13% of the structures observed with RanGTP were multipolar spindles. These RanGTP results are consistent with previous

work (Carazo-Salas *et al*., 1999; Wilde and Zheng, 1999; Ohba *et al*., 1999; Lau *et al*., 2009)

The addition of excess RanGTP to the extract is known to cause a release of spindle assembly factors from Importin β (reviewed in Dasso, 2001; Kalab and Heald, 2008). When this happens near chromatin, the spindles can be larger than normal because the spindle is no longer limited by the reach of RanGTP created by chromatin-bound RCC1 (Bischoff *et al*., 1991). Whether this effect could be due solely to the release of spindle assembly factors from Importin β or from Importin β and Transportin was yet to be determined.

In fact, if the potential mechanism where Transportin binds and inhibits SAFs were true, then the potential effect of RanGTP releasing spindle assembly factors from Transportin could be mimicked, at least partially, by addition of M9M. Indeed, by adding M9M to mitotic extract, we observed similar microtubule structures to the ones we obtained by adding excess RanGTP, although these similar structures are not in the identical proportions or sizes compared to those seen with addition of RanGTP. (Figure 13C).

A notable effect of RanGTP addition (10 μM) was that mitotic spindles, which had a similar bipolar shape to the ones in control conditions, seem to have a larger surface area (Figure 13C). We quantified the surface area of the spindles in the control (MBP; Figure 13A) condition and used it as a baseline of 100%. We then quantified the size of the "normal-shaped" spindles in both M9M and Ran-GTP conditions. Compared to normally shaped bipolar spindles in the control condition, the normally shaped bipolar spindles in the MBP-M9M (10 μM) condition were 140% larger, while the normal

bipolar spindles in the excess RanGTP (10 μM) condition were 170% larger (Figure 14). These results indicate that excess RanGTP and M9M have similar effects on mitotic *Xenopus* egg extract, although M9M has a slightly weaker effect than excess RanGTP.

To further explore this point, we tested the addition of M9M or excess RanGTP to a *Xenopus* CSF extract that did not contain chromatin. CSF extract supplemented with an ATP-regenerating system was incubated for one hour with rhodamine-labeled tubulin and either MBP (10 μM; control), RanQ69L-GTP (10 μM), or MBP-M9M (10 μM); the results were analyzed by fluorescence microscopy (Figure 15). In the control MBP condition, no microtubule structures were detected (Figure 15: +MBP). However, the addition of excess RanGTP or MBP-M9M caused aster formation (Figure 15: +Ran;+MBP). As seen in the previous experiment, the effect of excess RanGTP addition was stronger than that of M9M, with more and larger asters forming in the excess RanGTP than in the M9M condition.

This was the first piece of evidence suggesting that the Ran Titration Model is incorrect. If in mitosis, no spindle assembly cargoes exist for Transportin, then addition of M9M should have had no effect on microtubule structures. However, this was not what we observed. We found that addition of M9M produced both free asters and larger spindles around chromatin than in the control condition. Asters and larger spindles are similar to what was seen in the excess RanGTP condition, where we know that RanGTP is releasing SAFs from at least Importin β (Nachury *et al*, 2001). In the Direct Inhibition model, where Transportin binds to and regulates spindle assembly factors, the addition of either RanGTP or M9M would indeed cause an accumulation of freed SAFs. This could cause both the larger spindles and the spontaneous microtubule nucleation that results in

free asters. Since RanGTP would work on both the Transportin- and Importin β-bound SAFs, while M9M would free only Transportin-bound SAFs, it makes sense that in our experiments the excess RanGTP condition showed more and larger asters and spindles than the M9M condition.

Testing the Model of Action Through Use of TLB, a Mutant Form of Transportin

To further elucidate Transportin's mechanism of action, we performed an experiment similar to the above, but this time we added TLB, the mutant form of Transportin that is missing the H8 loop that allows it to bind RanGTP without displacing cargo. As before, we formed nuclei in an interphase *Xenopus* egg extract and allowed the DNA to replicate. We then added CSF extract, to convert the system to the mitotic state, and recombinant proteins as noted and observed the resulting microtubule structures (Figure 16; quantification of structures in Figure 17). In the control conditions, where either GST or MBP was added, almost 80% of structures observed over the chromatin were strong bipolar spindles (Figures 16 A&B). Addition of excess GST-Transportin (20 μM) caused a dramatic loss of spindle assembly over condensed chromatin (Figure 16C; as observed previously in Lau *et al* (2009). Notably, addition of GST-TLB (20 μM), the recombinant mutant Transportin, also clearly caused a loss of spindles (Figures 16D).

Addition of excess RanGTP in conjunction with excess GST-Transportin (10 μM and 20 μM, respectively) rescued spindle assembly, with 55% of condensed chromatin packages showing strong bipolar spindles (Figure 16E). This is consistent with our previous work (Lau *et al*., 2009). However, addition of excess RanGTP in conjunction with GST-TLB (10 μM and 20 μM, respectively) was unable to reverse the TLB block,

such that almost no condensed chromatin packages had strong bipolar spindles (Figure 16F). The Transportin-induced inhibition (20 μM) was reversed by addition of 10 μM RanGTP, whereas the TLB-induced inhibition (20 μM) was not. The 10 μM RanGTP concentration was chosen because 15-20 μM RanGTP addition was so potent that asters formed everywhere in the reaction and normal spindles of any type were rare, presumably due to the release of SAFs and subsequent microtubule nucleation everywhere, no only around chromatin (data not shown).

These results clearly argue against the Ran Titration Model, as excess RanGTP was unable to rescue TLB's inhibition of mitotic spindle formation. That is, if TLB were simply binding and sequestering RanGTP, thus depriving Importin β of a full complement of RanGTP, then addition of excess RanGTP should have allowed spindle assembly. But addition of excess RanGTP did not release the TLB inhibition.

Lastly, we found that the addition of M9M in conjunction with either Transportin or TLB was most illustrative. Specifically, the addition of M9M (10 μM) was actually able to rescue the effects of excess Transportin (20 μM) (Figure 16G). Over 65% of the condensed chromatin packages showed strong bipolar spindles. Intriguingly, M9M (10 μM) also rescued the inhibition by TLB (20 μM), with over 70% of the condensed chromatin packages showing strong bipolar spindles (Figure 16H).

The Direct Inhibition Model for Transportin's action in spindle assembly proposes that Transportin binds and masks spindle assembly factors everywhere but in the vicinity of chromatin. The reverse of TLB inhibition by M9M strongly implies that the recovery of spindles over condensed chromatin had to be caused by M9M blocking or reversing TLB's sequestration of SAFs. And because M9M has no effect on endogenous

Xenopus Importin β (as seen previously in this section), the effect seen can be solely attributed to the action of Transportin. This strongly argues that TLB, and therefore Transportin itself, acts in mitosis by binding and masking spindle assembly factors.

Discussion

The goal of this thesis was to provide evidence for the mechanism of action of Transportin in mitotic spindle assembly. Previously, it was found that Transportin has a negative regulatory role in the major mitotic assembly events: spindle assembly, nuclear membrane assembly, and nuclear pore assembly (Lau *et al*., 2009). However, Transportin's mechanism of action had yet to be elucidated. Transportin could function to titrate RanGTP and thus indirectly modulate the function of Importin β in mitotic events. Another possibility was that Transportin acts directly on spindle assembly factors by binding and ubiquitously masking one or more SAFs everywhere except in the vicinity of chromatin and RanGTP. To test these models, we used the synthetic signal peptide M9M, an inhibitor of Transportin, and the Transportin mutant TLB (Cansizoglu *et al*., 2007; Chook *et al*., 2002). We worked both *in vivo* in HeLa cells and *in vitro* in extracts derived from *Xenopus laevis* eggs.

We first quantified both endogenous Transportin and Importin-β in *Xenopus* egg extract by immunoblot analysis. We found that Transportin and Importin β had comparable endogenous concentrations (7uM and 6.5uM, respectively). Thus, the two receptors exist in comparable amounts, consistent with the findings that both receptors play significant roles in spindle assembly (Nachury *et al*., 2001; Gruss, *et al*., 2001; Lau *et al*., 2009).

We then verified that M9M interacted with Transportin but not Importin β. We looked at both the direct interactions, using recombinant proteins, and indirect interactions, using recombinant MBP constructs and endogenous Transportin and Importin β in *Xenopus* egg extracts. We determined that M9M interacts with both

recombinant and endogenous *Xenopus* Transportin, but not with Importin β, just as is true for mammalian Transportin and Importin β (Cansizoglu *et al*., 2007). Control reactions illustrated that the interaction between M9M and Transportin was specific.

Next, we examined the phenotypic effects on mitosis of inhibition of Transportin in HeLa cells. When HeLa cells were transfected with myc-tagged M9M, we observed striking defects on cytokinesis and spindle assembly, including an excess of microtubule midbodies, the appearance of DNA bridges, the production of multinucleate cells, and a predominance of abnormal spindles. Indeed, almost 30% of the total M9M-transfected cells showed a defect in either completion of mitosis or cytokinesis. We conclude that Transportin inhibition resulted in these significant defects and caused the cells to stop or be severely delayed at these points in the cell cycle. However, the direct cause of these *in vivo* defects is unclear, since Transportin also plays a significant role in nuclear import (Lau *et al*., 2009; Pollard *et al*, 1996). Thus, in this *in vivo* situation, we could not formally exclude the possibility that inhibiting Transportin stopped the *import* of potential spindle assembly factors or chromosomal proteins prior to mitosis, and thus caused the obvious later defects in mitosis and cytokinesis.

However, when M9M was added to *in vitro* spindle assembly assays performed in *Xenopus* egg extract, it clearly produced larger spindles than those seen in the control condition, similar to the ones we and others have observed with the addition of excess RanGTP. Moreover, we observed that M9M produced free asters, albeit smaller, to those produced in excess RanGTP conditions, both in chromatin-plus and chromatin-minus conditions. This suggested that M9M was acting by inhibiting the binding of spindle assembly factors by Transportin, thus freeing the SAFs for spindle and aster assembly

Finally, we used TLB, the mutant form of Transportin that is desensitized to RanGTP-mediated cargo release, with *Xenopus* egg extract to observe how inhibition of Transportin's ability to release cargo affected spindle assembly. Adding TLB to the extract inhibited spindle assembly. Importantly, we found that this effect was not rescued by excess RanGTP addition. These results are completely inconsistent with a Ran Titration Model.

However, addition of M9M with TLB to the spindle assembly assay gave the most definitive result. Adding M9M and TLB showed a recovery of the spindle formation around condensed chromatin. M9M is known to block TLB's ability to bind cargo, but has no impact on interactions between TLB and RanGTP (Cansizoglu *et al*., 2007). Thus, rescue of spindle assembly by M9M must be due to M9M blocking TLB from sequestering spindle assembly factors. We thus conclude that Transportin acts in mitosis, not by indirectly regulating Importin β through RanGTP titration, but by binding and masking spindle assembly factors.

In other work in the lab, the role of Transportin in regulating post-mitotic nuclear assembly and nuclear pore assembly is being tested. Currently, we have found evidence similarly supporting a Direct Inhibition Model for nuclear assembly (Bernis, unpublished work). We thus believe that Transportin functions directly in nuclear assembly by inhibiting a subset of nuclear pore proteins everywhere except in the vicinity of chromatin, and indeed Transportin has been shown to bind multiple nuclear pore proteins (Lau *et al*., 2009). Additionally, we are doing experiments will determine whether Transportin functions to regulate nuclear membrane assembly directly or indirectly.

In the future, a strong supporting piece of evidence for the Direct Inhibition mechanism of action for Transportin would be identification of a target of Transportin that is a spindle assembly factor. However, this is not as easy at it seems. Because of the variability of the PY-NLS, simple bioinformatics cannot be the only tool used to find these targets. Additionally, not every spindle assembly factor has been found and sequenced, so it is possible that at least some spindle assembly factor targets for Transportin are as yet undiscovered proteins. Also, it is difficult to distinguish between interphase and mitotic targets in an experiment such as an immunoprecipitation – it will be possible to find many targets of Transportin, but delineating which of these targets are known nuclear import targets and which are possible spindle assembly factors will be more difficult.

However, experiments to determine possible mitotic targets of Transportin are under way. We are currently looking at the spindle assembly factor targets of Importin β, such as the ones delineated in Kalab *et al* (2008), to determine if any of these targets have PY-NLSs. Transportin and Importin β might serve in parallel in order to regulate these spindle assembly factors. Of interest in this case is the fact that we have previously demonstrated that the Nups regulated by Importin β and Transportin during nuclear assembly are, to date, almost completely overlapping (Lau *et al*, 2009). Currently, we are also determining whether some of the known spindle assembly factors with PY-NLSs, such as Nup98, interact with Transportin (Fontoura *et al*., 2000; Cross and Powers, 2011). Also of interest are the other key components of the nuclear pore that are known to interact with Transportin: the Nup107-160 complex and the pore-initiating protein ELYS (Lau *et al*., 2009). The Nup107-160 complex is a set of interacting nucleoporins

that localize to kinetochores during mitosis and are required for spindle assembly (Orjalo *et al*., 2006). ELYS, which also localizes to kinetochores in mitosis, is essential for both completion of cytokinesis and proper nuclear pore assembly (Rasala *et al*., 2006). These are promising targets.

In conclusion, we have strong evidence that Transportin does not act to titrate RanGTP, but has a more direct effect in regulating mitotic spindle assembly. We support the hypothesis that rather than modulating RanGTP, Transportin acts to bind and mask spindle assembly factors to ensure that the mitotic spindle forms only around chromatin.

Chapter 1 is currently being prepared for submission for publication. Bernis, Cyril; Swift-Taylor, Mary Elizabeth; Forbes, Douglass J. "Characterization of the Mechanism of Action of Transportin in Mitotic Spindle Assembly." I am a co-author in this publication.

Figures

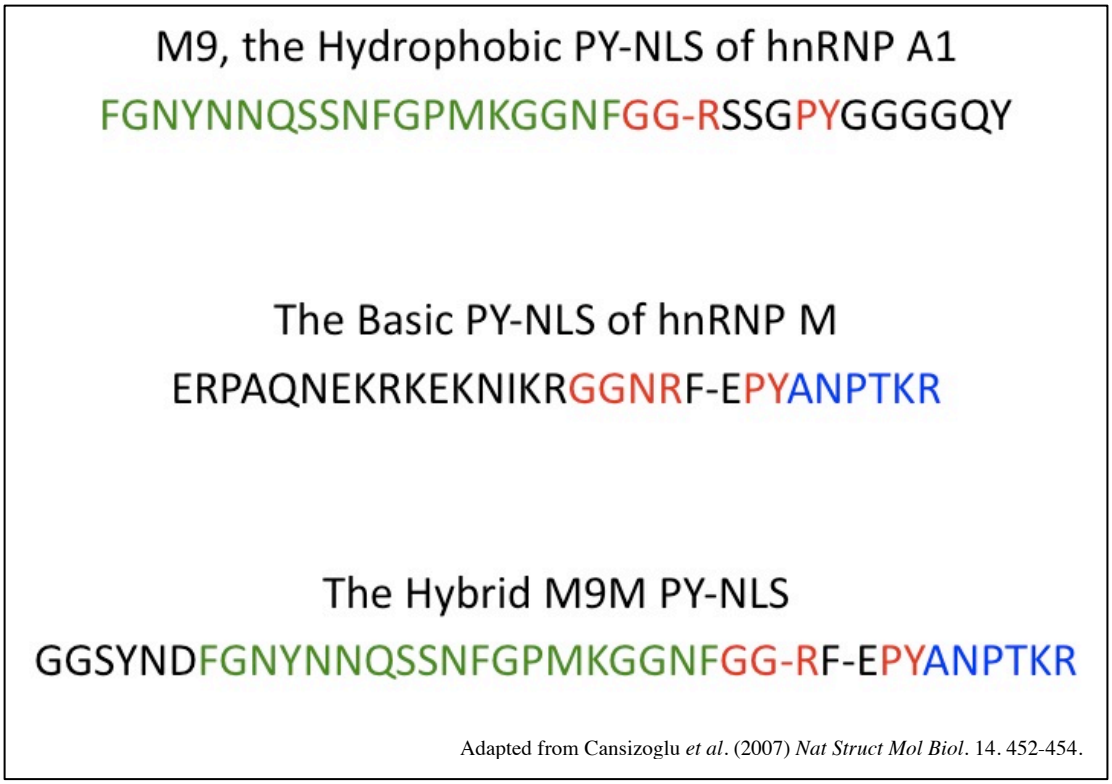

Figure 5 – M9M, A Synthetic Hybrid PY-NLS Peptide Capable of Binding to Transportin with 200 fold Binding Strength

M9 is the nuclear localization signal (NLS) found in hnRNP A1; it is in the class of hydrophobic PY-NLSs. Next shown is the basic PY-NLS found in hnRNP M. M9M is a hybrid constructed from these hydrophobic and basic PY-NLSs. In subsequent experiments, MBP-M9M is used as the recombinant form of M9M, where M9M is fused to maltose binding-protein (MBP) for ease of purification and use.

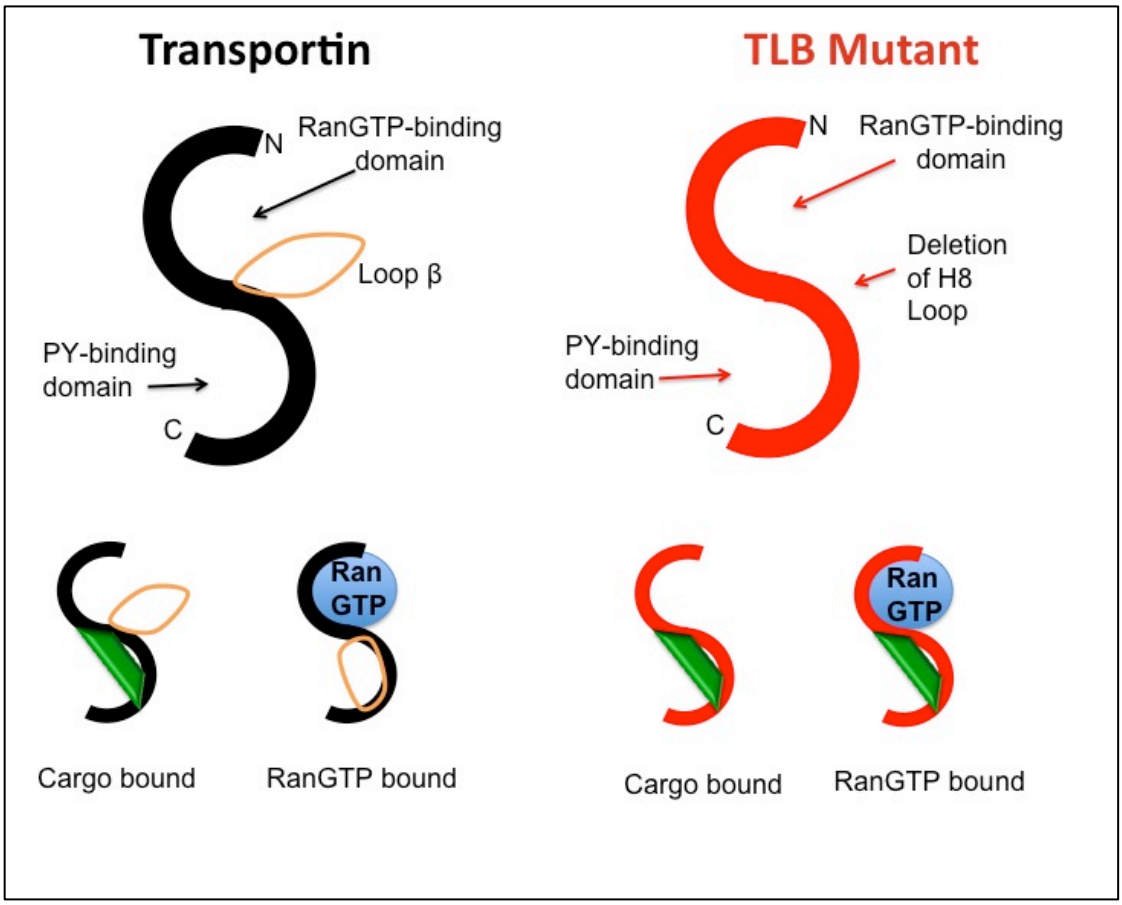

Figure 6 – TLB is a Mutant Form of Transportin with a Truncated H8 Loop, Preventing Cargo Displacement by RanGTP
Wild-type Transportin recognizes and binds cargo containing a PY-NLS. When the Transportin:cargo complex encounters RanGTP, Transportin will bind the RanGTP, and the H8 loop will move to displace the cargo. The Transportin TLB mutant lacks the H8 loop, and as such when RanGTP interacts with the cargo-laden complex, the cargo is not displaced. This allows TLB to be bound to both cargo and RanGTP simultaneously.

This schematic representation is an adaption of the description provided in Chook *et al*. (2002). *Biochem*. 41. 6955-6966.

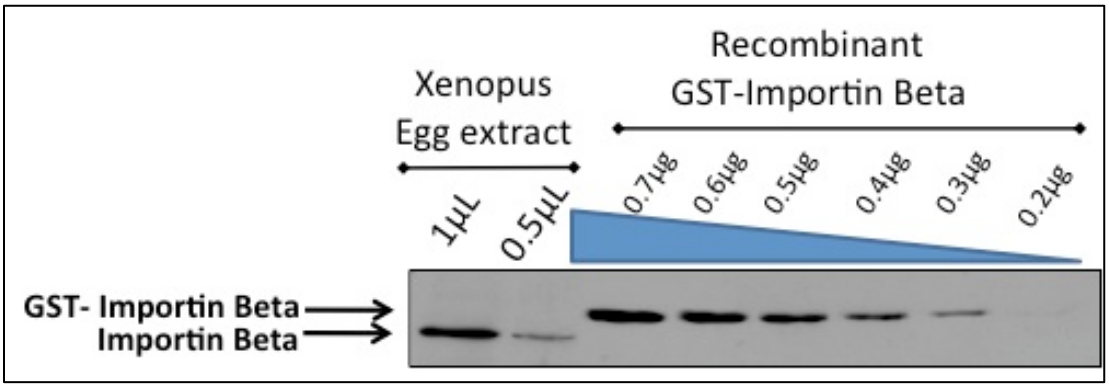

Figure 7 – Quantitation of the Endogenous Importin β Concentration in *Xenopus* Interphase Egg Extract via Immunoblot

The quantity of Importin β in *Xenopus* egg extracts (1 µL and 0.5 µL) was compared to a set of sequentially diluted standards made of recombinant GST-tagged *Xenopus* Importin β (0.7 µg - 0.2 µg) by immunoblot using an anti-*Xenopus* Importin β antibody (Delmar *et al.*, 2008). Using ImageJ software to objectively quantify the bands, we determined that 1 µL of extract contains Importin β comparable to 0.6 µg GST-Importin β. This was an average of three such experiments; a representative image is shown here. GST-Importin β is approximately 126 kD in size, which gave a concentration of Importin β in the extract of approximately 4.5 µM.

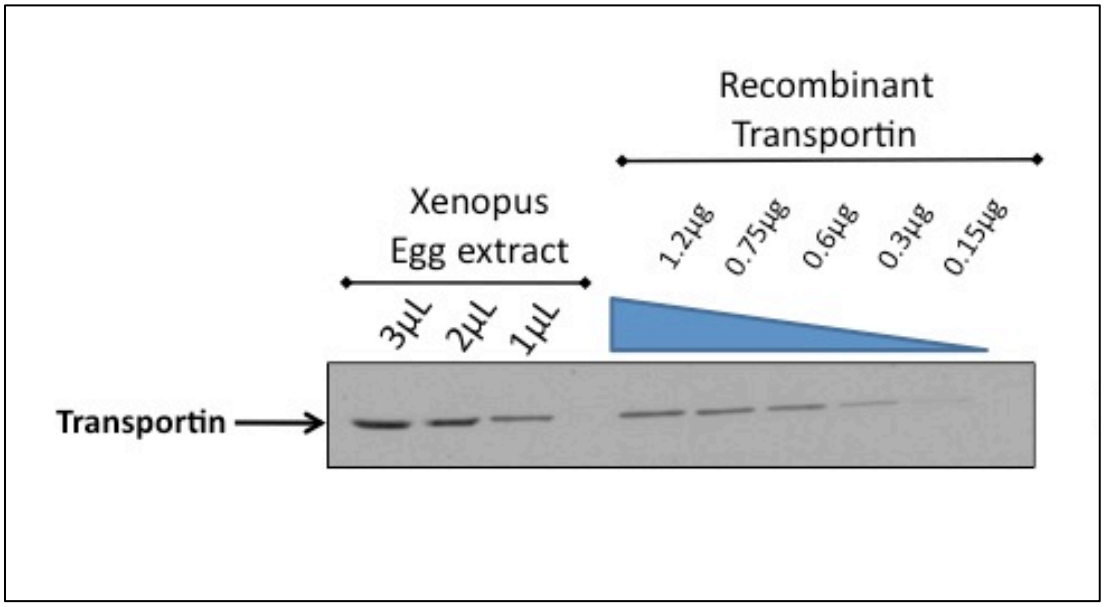

Figure 8 – Quantitation of Endogenous Transportin Concentration in *Xenopus* Interphase Egg Extract via Immunoblot

The quantity of Transportin in *Xenopus* egg extracts (3 µL – 1 µL) was compared to a set of sequentially diluted standards made of recombinant untagged human Transportin (1.2 µg -0.15 µg) by immunoblot using an anti-hTransportin antibody (BD Biosciences, San Jose, CA). Using ImageJ software to objectively quantify the bands, we determined that 1 µL of extract contains Transportin comparable to the 0.65 µg of recombinant Transportin band. Untagged Transportin is approximately 92 kD in size, giving a concentration of Transportin in the extract of approximately 7 µM.

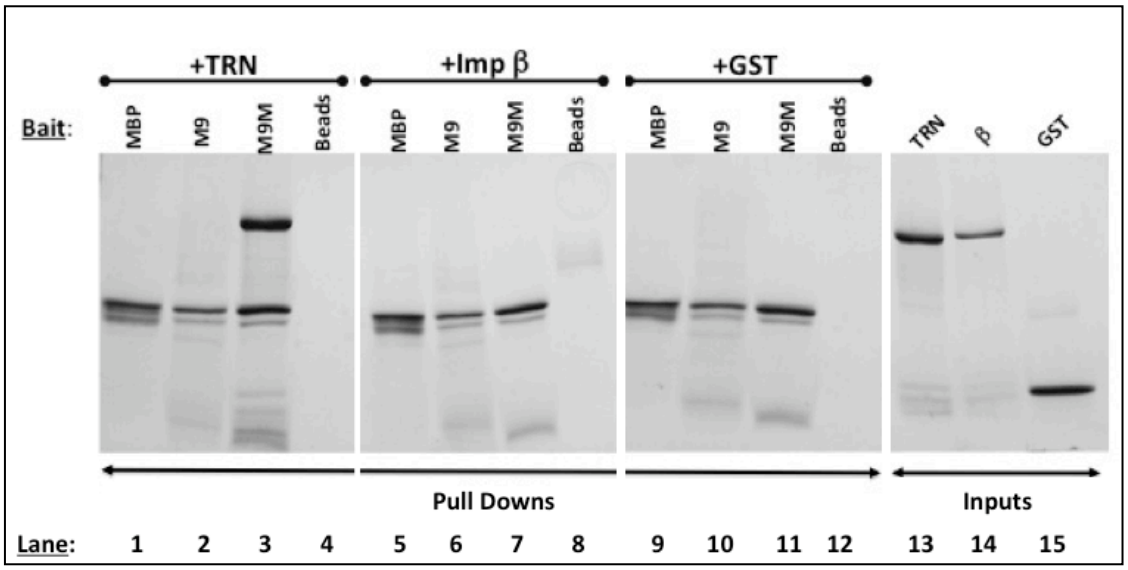

Figure 9 – M9M Interacts Directly with Transportin but Not with Importin β
Direct interaction pulldown experiments were performed in order to detect interactions between recombinant MBP constructs (MBP, MBP-M9, MBP-M9M) and GST constructs (GST, GST-Transportin, GST-Importin-β). The MBP (130 μg) constructs were individually bound to amylose beads for 40 minutes and the beads were subsequently blocked with 2 mg bovine serum albumin (BSA). After washing away unbound proteins, each set of beads (MBP, MBP-M9, or MBP-M9M) was then incubated with a 100 μg of GST, GST-Transportin, or GST-Importin β for 1 hour. After washing away unbound proteins, the bound GST proteins were eluted from the beads and the results run on PAGE-SDS, along with samples of the GST constructs for comparison. It can be seen that GST-Transportin (lane 3), but not Importin β (lane 7), interacts with MBP-M9M. Importantly, MBP-M9M does not interact with GST alone (lane 11) and GST-Transportin does not interact with MBP alone (lane 1).

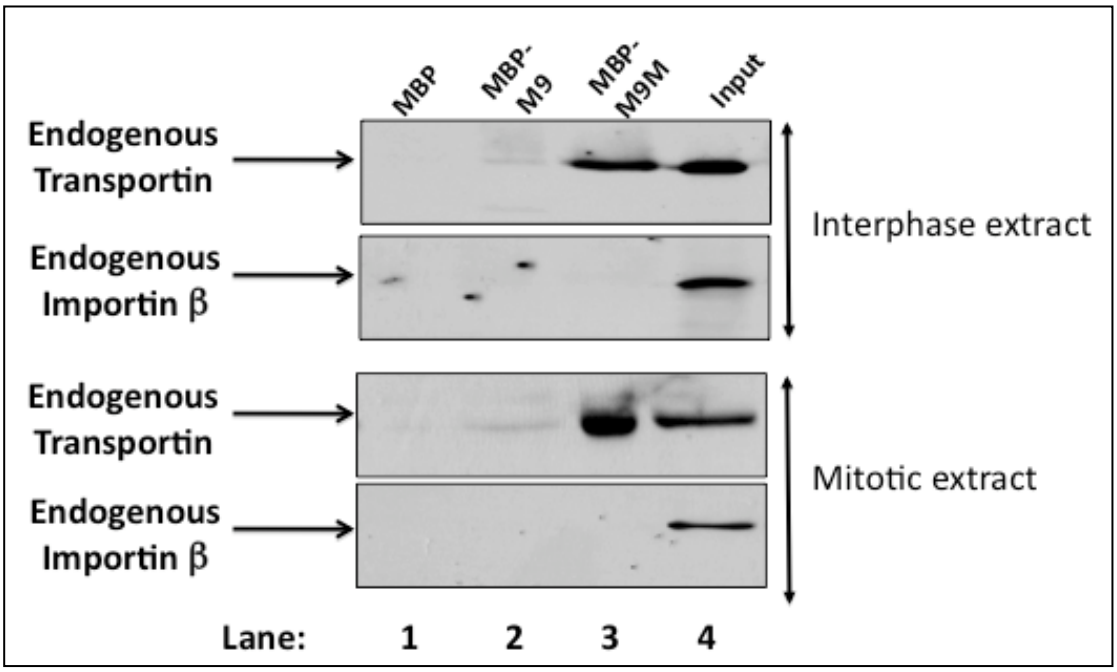

Figure 10 - M9M Binds Endogenous *Xenopus* Transportin But Not Endogenous Importin β

Recombinant MBP constructs (130 µg MBP, MBP-M9, or MBP-M9M) were incubated with amylose beads for 40 minutes. The beads were subsequently blocked with 2mg bovine serum albumin for 20 minutes and then unbound proteins were washed away. Each set of beads was then incubated with 100 µL of either mitotic (CSF) or interphase extract for 1 hour. After washing away the unbound extracts, the constructs were eluted from the beads and the results were processed via PAGE-SDS and immunoblotted with either mouse anti-hTransportin (BD Biosciences, San Jose, CA) or anti-Xenopus Importin β (Rasala, 2006).

In both extracts, MBP was not able to pull down endogenous *Xenopus* Transportin or Importin-β and MBP-M9 was able to only pull down a very small amount of endogenous Transportin. MBP-M9M was able to pull down a significant amount of endogenous Transportin but no Importin β. This indicates that, in both mitotic and interphase extract, MBP interacts with neither receptor, M9 mildly interacts with endogenous Transportin, and M9M interacts strongly with Transportin and not Importin β.

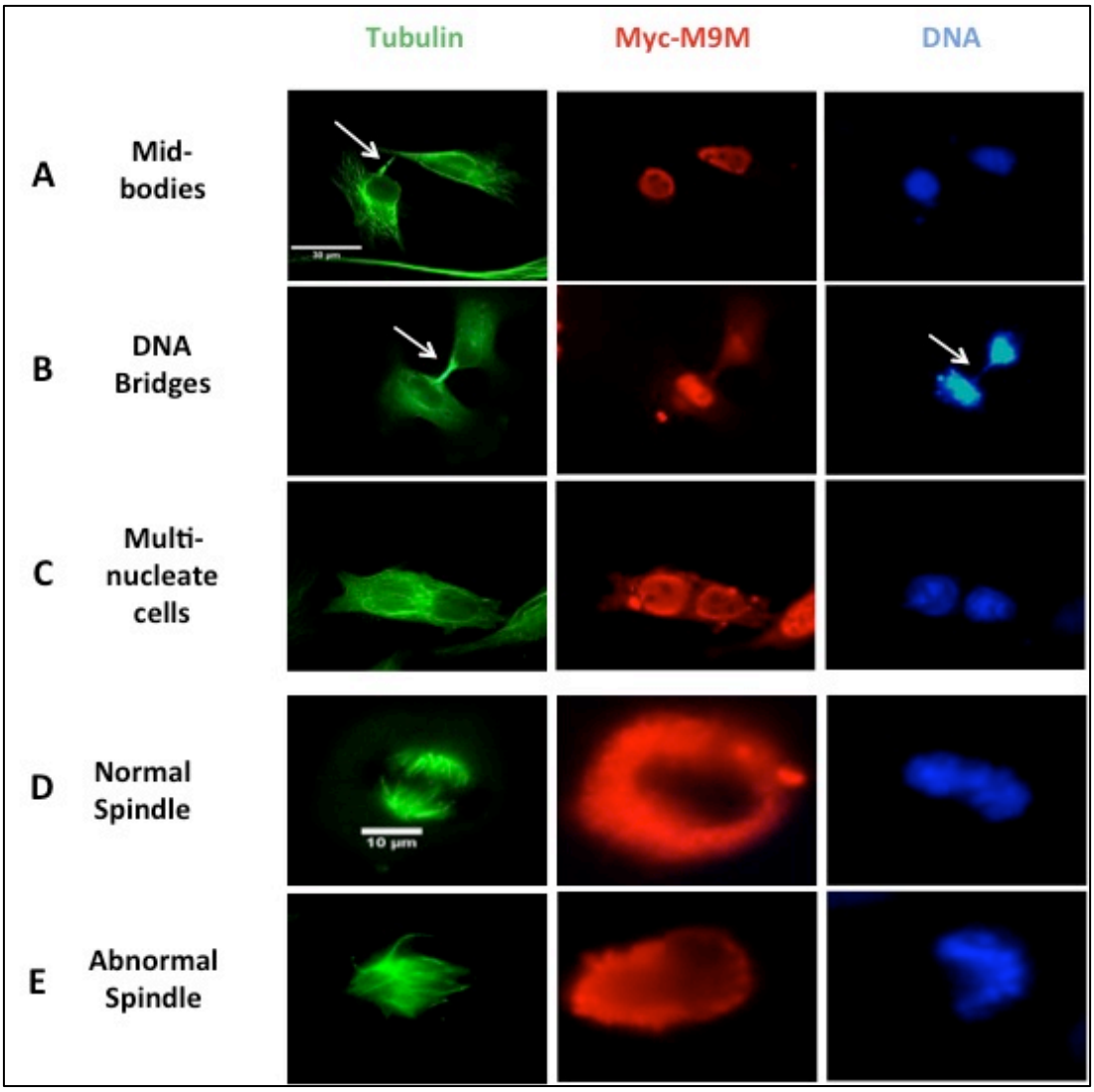

Figure 11 – M9M Inhibition of Transportin Causes Defects in Mitosis

HeLa cells were transfected for 24 hours with mammalian expression vectors containing myc-tagged MBP constructs (MBP, MBP-M9, MBP-M9M). The transfection of the M9M construct caused clear defects in cytokinesis. Abnormal structures observed included: (A) excess midbodies, (B) DNA bridges between cells accompanying said midbodies, and (C) multinucleate cells. In addition, of the cells showing mitotic spindles, a large fraction had defective spindles (D) after MBP-M9M construct transfection. Few of these defects were seen in cells that were either not transfected or transfected with myc-tagged MBP or myc-tagged MBP-M9. Tubulin is visualized in green with a FITC-labeled anti-tubulin antibody (green), transfected cells are visualized with a TRITC-labeled anti-myc antibody (red), and DNA is visualized with DAPI (blue).

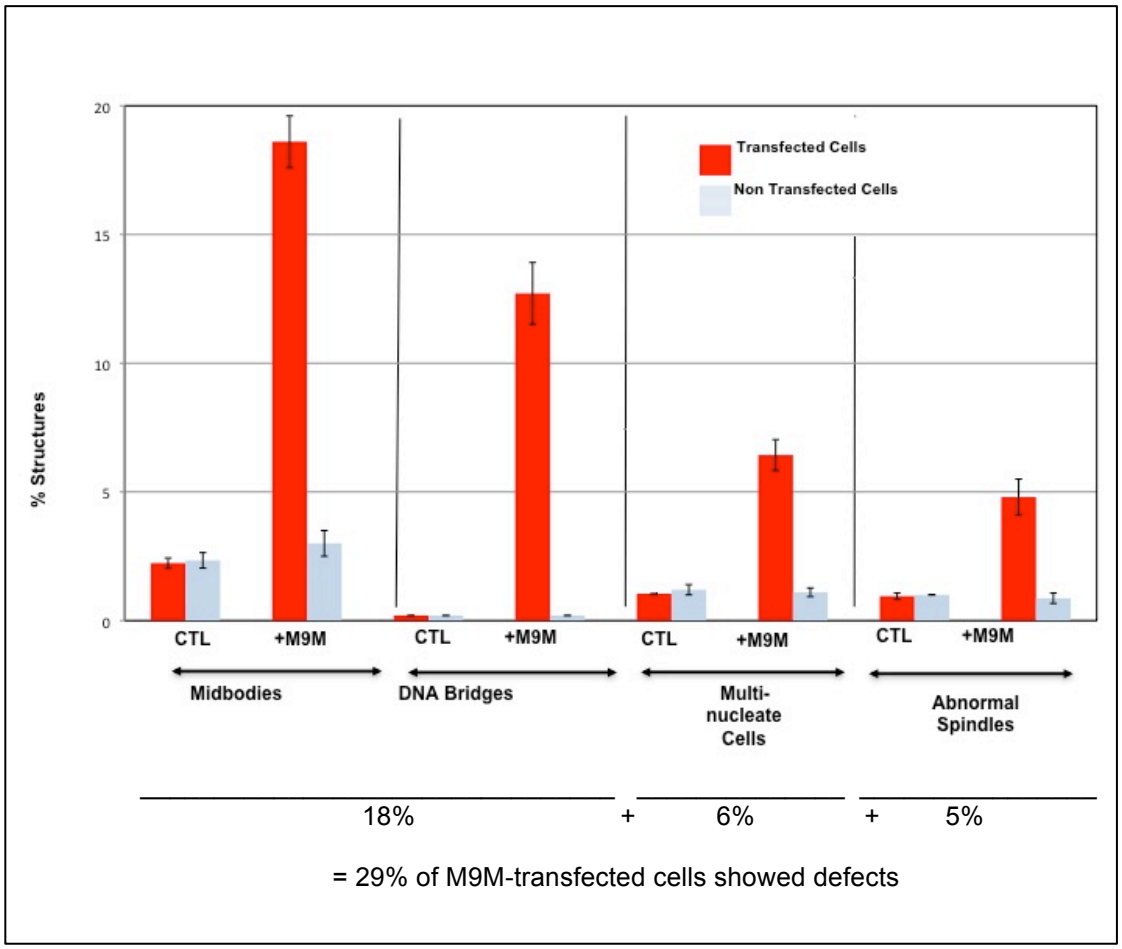

Figure 12 – Quantitation of Aberrant Structures Seen in HeLa Cells Transfected with MBP Constructs

Cells transfected with MBP-M9M show clear defects in cytokinesis and mitosis. Transfected cells were detected using an antibody to the myc-tag in the construct (TRITC anti-myc), causing cells that took up the construct to appear red. Microtubules were visualized using an antibody to tubulin (FITC anti-tubulin), making microtubule structures appear green. In cells transfected with MBP-M9M, 18% showed midbodies, as compared to less than 3% of non-transfected cells and cells transfected with MBP (control). 13% of the MBP-M9M transfected cells showed both microtubule midbodies and DNA bridges, as opposed to almost none in the control or non-transfected cells. 6% of the MBP-M9M transfected cells were multinucleate, as opposed to less than 1% of control and non-transfected cells. In all transfections, 6% of the total cells had mitotic spindles, normal or abnormal. 5% of the total MBP-M9M transfected cells showed abnormal spindles, whereas less than 1% of the total control or non-transfected cells had abnormal spindles.

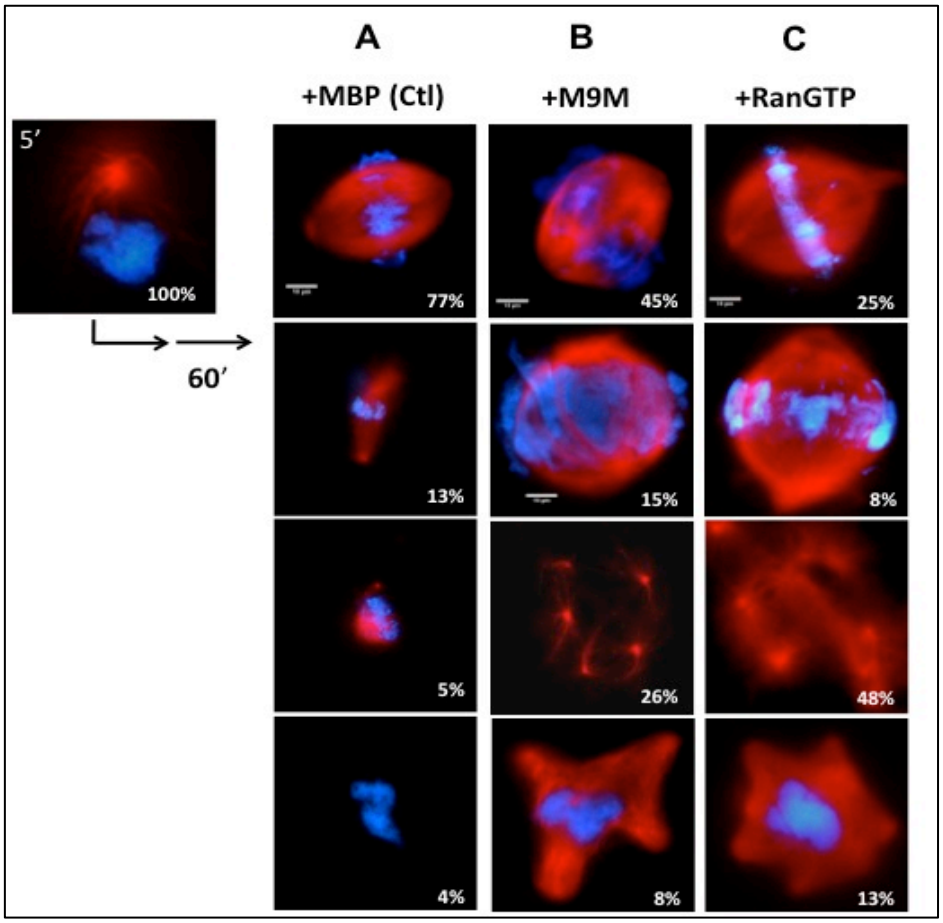

Figure 13 – Effects of M9M and RanGTP on *In Vitro* Spindle Assembly

Freshly prepared interphase *Xenopus* egg extract was mixed with sperm chromatin and rhodamine-labeled tubulin; nuclei were allowed to form and the DNA was allowed to replicate for one hour. A portion of this reaction was added to mitotic *Xenopus* extract to convert it entirely to a mitotic state and recombinant proteins were added as noted. The resulting microtubule structures were examined using immunofluorescence microscopy. The microtubules are seen as red due to the integration of the rhodamine-labeled tubulin into normal microtubule structures and the chromatin is blue due to the Hoescht DNA stain.

A - Control condition, 10 μM MBP. The majority (77%) of condensed chromatin contained microtubule structures that formed strong bipolar spindles. Also seen were weak spindles (13%), half spindles (5%), and no microtubule activity (4%) **B** – 10 μM MBP-M9M. 45% of structures were normally shaped, albeit larger, bipolar spindles over condensed DNA. 15% of structures were very large bipolar spindles over a more-than-normal amount of DNA. 26% of structures were asters with no associated chromatin. These were smaller than the asters formed in the RanGTP condition. 8% of structures in the M9M condition were multipolar spindles. **C** – 10 μM RanQ69L loaded with GTP. 25% of microtubule structures were normal, albeit smaller, bipolar spindles, while 8% had much more DNA associated with much larger spindles. 48% of structures were large asters with no associated chromatin, and 13% were multipolar spindles.

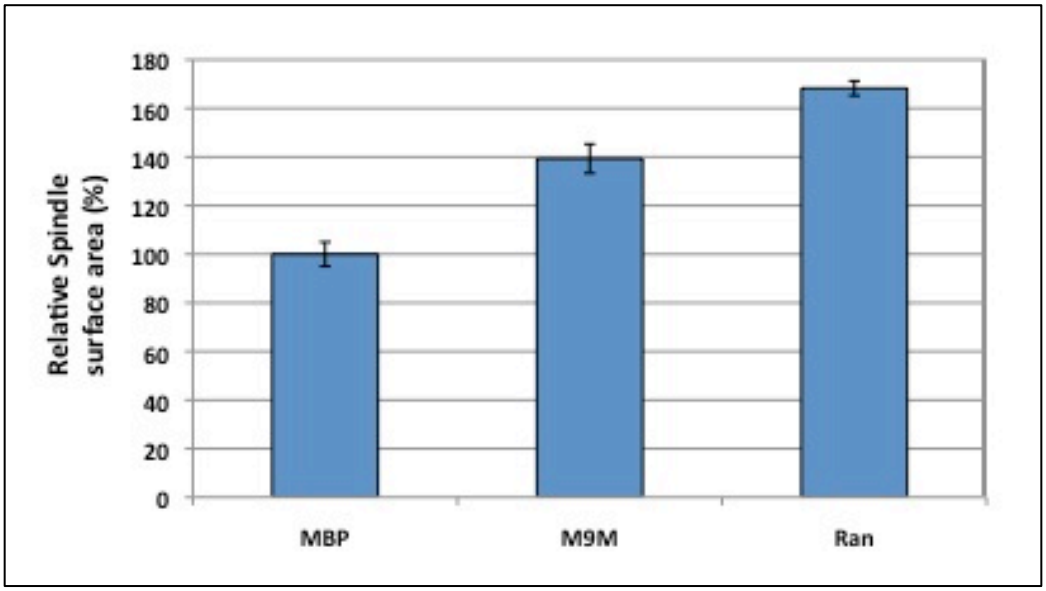

Figure 14 – M9M, like RanGTP, Promotes Larger Spindles *In Vitro*
The surface area of the normally shaped bipolar spindles from the MBP, M9M, and RanGTP conditions in Figure 12 (top panels) were measured using ImageJ software. Overall, the bipolar spindles were much larger in the MBP-M9M condition than in the MBP condition, and the RanQ69LGTP-condition bipolar spindles were even larger. This may be due to M9M blocking the sequestration of spindle assembly factors by endogenous Transportin, and RanGTP causing release of spindle assembly factors from both Transportin and Importin-β.

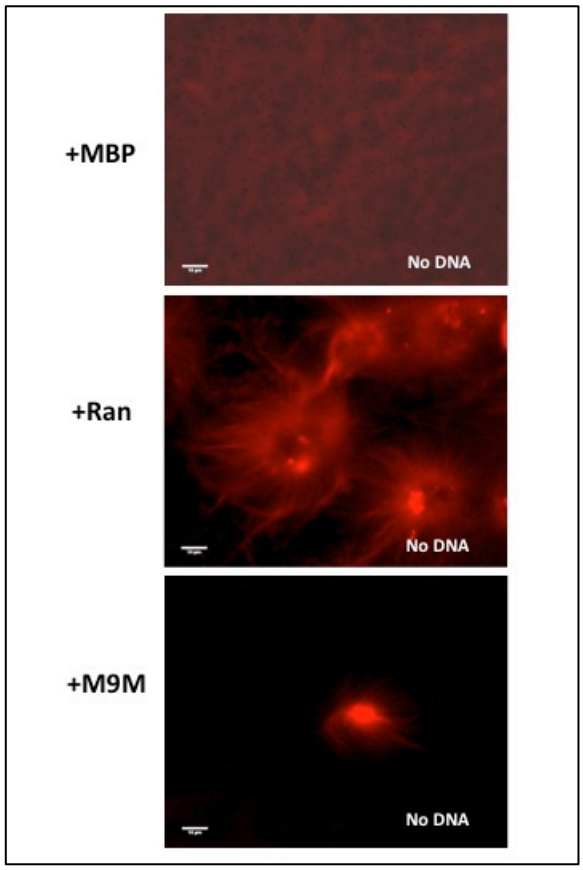

Figure 15 – In the Absence of Chromatin, M9M, like RanGTP, Induces Aster Assembly

Xenopus extract was incubated with energy mix, rhodamine-labeled tubulin, and 10 μM MBP (control), 10 μM RanQ69L-GTP, or 10 μM MBP-M9M, all without chromatin. No microtubule structures were observed in the control condition. As previously shown, RanGTP induced formation of microtubule asters. This can be explained as RanGTP causing the release of spindle assembly factors from Importin-β, causing impromptu microtubule nucleation (Nachury *et al.,* 2001; Gruss *et al.*, 2001). Interestingly, microtubule asters also formed when MBP-M9M was present in the absence of chromatin. Since MBP-M9M can only work on Transportin, this supports the idea that Transportin is binding and masking spindle assembly factors on its own, and thus when M9M prevents Transportin from binding cargo, these spindle assembly factors are unmasked and cause impromptu microtubule nucleation, i.e., asters.

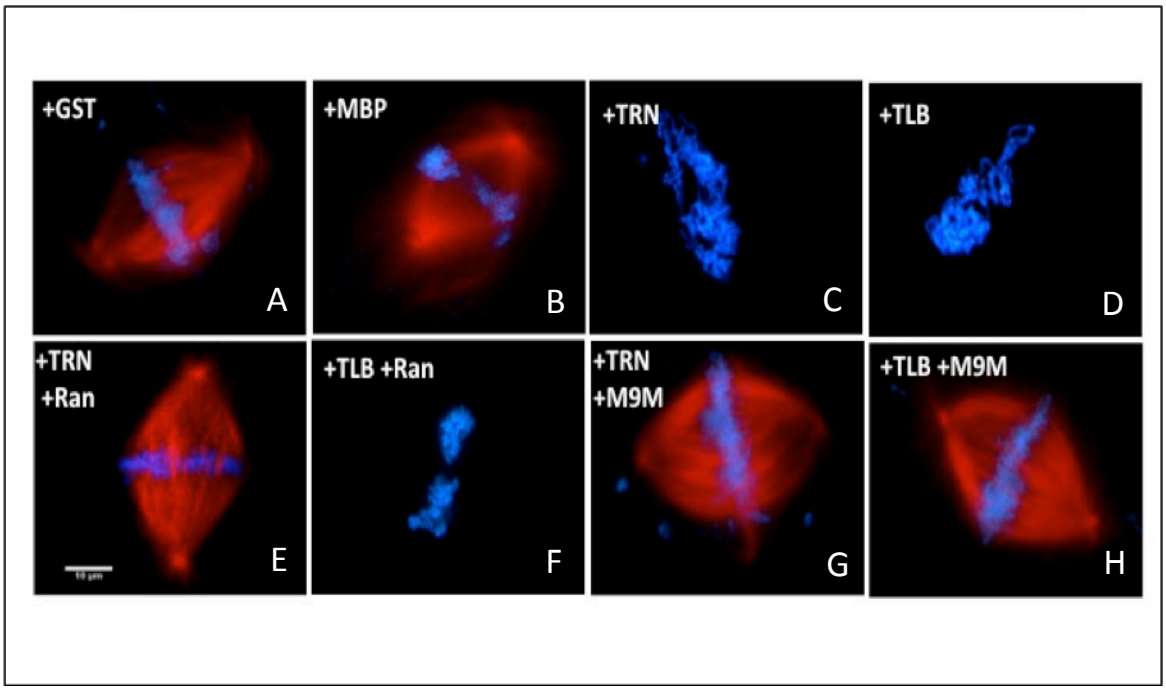

Figure 16 – TLB Inhibition of Spindle Assembly Cannot be Reversed by Excess RanGTP but Can be Blocked by M9M

Interphase *Xenopus* egg extract was mixed with sperm chromatin and rhodamine-labeled tubulin; nuclei were allowed to form and the DNA was allowed to replicate for one hour. A portion of this reaction was added to mitotic *Xenopus* extract to convert the entity to a mitotic state. Recombinant proteins were added as noted. The resulting microtubule structures were examined under a microscope using immunofluorescence microscopy, where the microtubules are red due to the integration of rhodamine-labeled tubulin into normal mitotic structures and the chromatin is blue due to Hoescht DNA stain in the buffer used to fix the structures. Representative images are shown.

A & B – 20 μM GST or 10 μM MBP are controls, showing normal bipolar spindles. **C & D** – 20 μM GST-Transportin or 20 μM GST-TLB showed almost no microtubule formation over chromatin. **E** – 10 μM RanQ69LGTP and 20 μM GST-Transportin; rescue of normal bipolar spindles (as shown in *Lau, 2009*). **F** – 10 μM RanQ69L-GTP and 20 μM GST-TLB; no microtubule formation over chromatin. **G** - 10μM MBP-M9M and 20 μM GST-Transportin; rescue of robust bipolar spindles. **H** – 10 μM MBP-M9M and 20 μM GST-TLB; rescue of robust bipolar spindles.

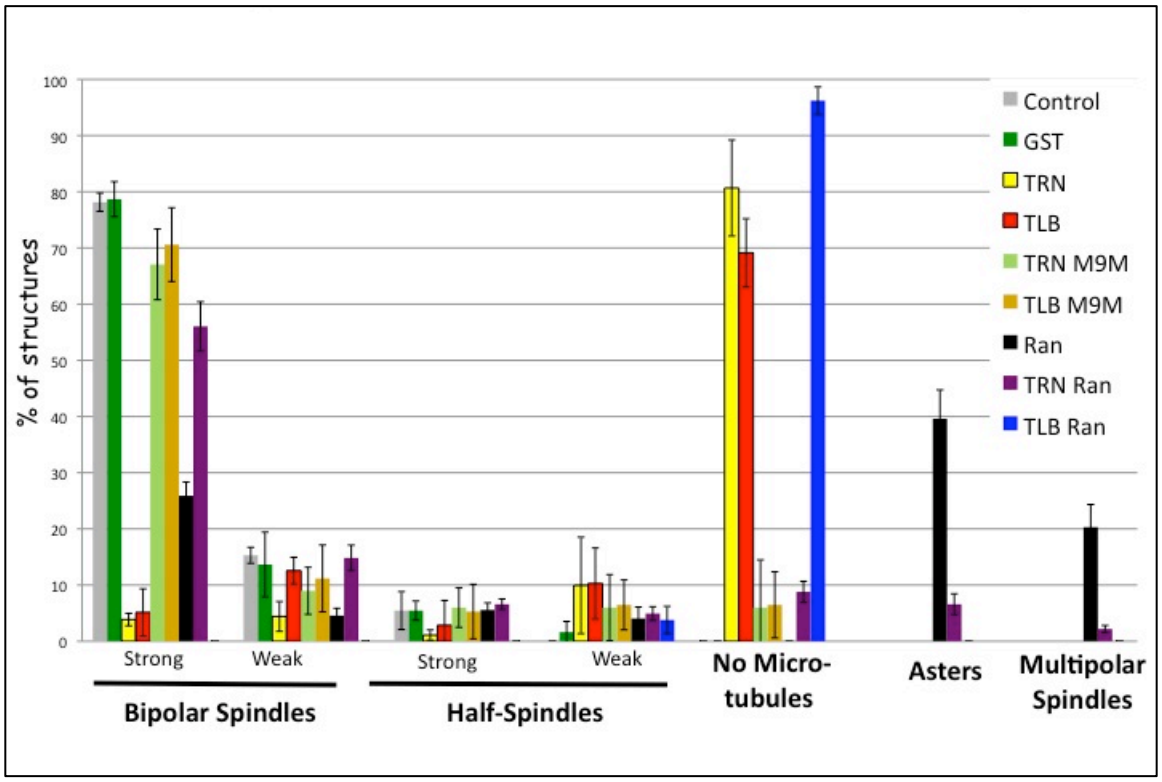

Figure 17 – Quantitation of the Effects of TLB, Excess Transportin, M9M, and RanGTP on Spindle Assembly

Coverslips from the experiment shown in Figure 16 were examined and the structures seen were quantified. Control conditions (10 µM MBP or 20 µM GST) had almost 80% normal bipolar spindles. Addition of 20 µM GST-TLB or 20 µM GST-Transportin to extract caused a dramatic loss of spindle formation, down to 5% or less in these experimental conditions. Addition of 10µM excess RanQ69L-GTP with 20 µM GST-Transportin rescued this to approximately 55% normal spindles. However, the 10 µM excess RanQ69L-GTP with 20 µM GST-TLB condition showed no increase in spindle formation (less than 5% normal bipolar spindles). Addition of 10 µM MBP-M9M with 20 µM GST-Transportin rescued normal bipolar spindles over 65%. Addition of 10 µM MBP-M9M and 20 µM GST-TLB was also rescued to over 70% normal bipolar spindles.

References

Allen, T.D., Cronshaw, J.M, Bagley, S., Kiseleva, E., Goldberg, M.W. (2000). The nuclear pore complex: mediator of translocation between nucleus and cytoplasm. J. Cell Sci. *113*, 1651–1659.

Andrade, M.A. and Bork, P. (1995). HEAT repeats in the Huntington's disease protein. Nat Genet *11*, 115-116.

Bayliss, R., Littlewood, T., Stewart, M. (2000). Structural basis for the interaction between FxFG nucleoporin repeats and importin-beta in nuclear trafficking. Cell *102*, 99-108.

Bischoff, F.R. and Ponstingl, H. (1991). Catalysis of guanine nucleotide exchange on Ran by the mitotic regulator RCC1. Nature **354**, 80–82

Bischoff, F.R., Klebe, C., Kretschmer, J., Wittinghofer, A. and Ponstingl, H. (1994). RanGAP1 induces GTPase activity of nuclear Ras-related Ran. Proc. Natl. Acad. Sci. U.S.A. **91**, 2587–2591

Blissenbach, M., Grewe, B., Hoffmann, B., Brandt, S., Uberla, K. (2010). Nuclear RNA Export and Packaging Function of HIV-1 REV Revisited. J Virol. *13*, 6598-6604.

Cansizoglu, A.E. and Chook, Y.M. (2007). Conformational heterogeneity of karyopherinβ2 is segmental. Structure *15*, 1431-1441.

Cansizoglu, A.E., Lee, B.J., Zhang, Z.C., Fontoura, B.M.A., Chook, Y.M. (2007). Structure-based design of a pathway-specific nuclear import inhibitor. Nat. Struct. Mol. Biol. *14*, 452-454.

Carazo-Salas, R.E. Guarguaglini, G., Gruss, O.J., Segref, A., Karsenti, E., Mattaj, I.W. (1999). Generation of GTP-bound Ran by RCC1 is required for chromatin-induced mitotic spindle formation. Nature 400, 178-181.

Chan, R.C, and Forbes, D.J. (2006). In Vitro Study of Nuclear Assembly and Nuclear Import Using Xenopus Egg Extracts. In Methods in Molcular Biology: Cell Biology and Signal Transduction. Liu X. Johne eds., (Totowa, NJ: Humana Press Inc.) pp. 289-300.

Chook, Y.M. and Blobel, G. (1999). Structure of the nuclear transport complex karyopherin-β2-RanGppNHp. Nature *399*, 230-237.

Chook, Y.M. and Suel, K.E. (2010). Nuclear import by karyopherin-βs: Recognition and inhibition. Biochim Biophys Acta [E*pub ahead of print]*

Chook, Y.M., Blobel, G. (2001). Karyopherins and nuclear import. Curr Opin Struct Biol *11*, 703-715.

Chook, Y.M., Jung, A., Rosen, M.K., Blobel, G. (2002). Uncoupling Kapβ2 substrate dissociation and ran binding. Biochem *41*, 6955-6966.

Clarke, P. R., and Zhang, C. (2008). Spatial and temporal coordination of mitosis by Ran GTPase. Nat. Rev. Mol. Cell Biol. *9*, 464–477.

Conti, E., Uy, M., Leighton, L., Blobel, G., Kuriyan, J. (1998). Crystallographic analysis of the recognition of a nuclear localization signal byt the nuclear import factor karyopherin alpha. Cell *94,* 193-204.

Cook, A., Bono, F., Jinek, M., and Conti, E. (2007). Structural biology of nucleocytoplasmic transport. Annu. Rev. Biochem. *76*, 647–671.

Cook, A.G. and Conti, E. (2010). Nuclear export complexes in the frame. Curr Opin Struct Biol *20*, 247-252.

Cronshaw, J.M., Krutchinsky, A.N., Zhang, W., Chait, B.T., Matunis, M.J. (2002). Proteomic analysis of the mammalian nuclear pore complex. J Cell Biol *158*, 915-927.

Cross, M.K. and Powers, M.A. (2011). Nup98 regulates bipolar spindle assembly through association with microtubules and opposition of MCAK. Mol Biol Cell *22*, 661-672.

Dasso, M. (2001). Running on Ran: nuclear transport and the mitotic spindle. Cell 104, 321-324.

Delmar, V.A., Chan, R.C, Forbes, D.J. (2008). Xenopus importin beta validates human importin beta as a cell cycle negative regulator. BMC Cell Biol *9*, 14.

Desai, A., Murray, A., Mitchison, T.J., Walczak, C.E. (1999). The use of *Xenopus* egg extracts to study mitotic spindle assembly and function in vitro. Methods Cell Bio. *61*, 385-412.

Dormann, D., Rodde, R., Edbauer, D., Bentmann, E., Fischer, I., Hruscha, A., Than, M.E., Mackenzie, I.R.A., Capell, A., Schmid, B., Neumann, M., Haass, C. (2010). ALS-associated fused in sarcoma (FUS) mutation disrupt Transportin-mediated nuclear import. EMBO *29*, 2841-2857.

Feldherr, C.M., Kallenbach, E., Schultz, N. (1984). Movement of a karyophilic protein through the nuclear pores of oocytes. J Cell Biol *99*, 2216-2222.

Fontoura, B.M.A., Blobel, G., Yaseen, N.R. (2000). The nucleoporin Nup98 is a site for GDP/GTP exchange on Ran and Termination of karyopherin beat2-mediated nuclear import. J Biol Chem *275*, 31289-31296.

Forbes, D.J., Kirschner, M.W., and Newport, J.W. (1983). Spontaneous Formation of Nucleus-like structures around bacteriophage DNA microinjected into *Xenopus* eggs. Cell *34*, 13-23.

Frey, S., Richter, R.P., Gorlich, D. (2006). FG-rich repeats of nuclear pore proteins for a three-dimensional meshwork with hydrogel-like properties. Science *314*, 815-817.

Fried, H., Kutay, U. (2003). Nucleocytoplasmic transport: taking an inventory. Cell Mole Life Sci *60*, 1659-1688.

Gorlich, D. and Kutay, U. (1999). Transport between the cell nucleaus and the cytoplasm. Annu Rev Cell Biol *15,* 607-660.

Gorlich, D., Kostka,S., Kraft,R.. Dingwall,C., Laskey,R.A., Hartmann,E., Prehn,S. (1995). Two different subunits of importin cooperate to recognize nuclear localization signals and bind them to the nuclear envelope. Curr Biol. *5*, 383-392.

Gorlich, D., Prehn, S., Laskey, R.A., Hartmann, E. (1994). Isolation of a protein that is essential for the first step of nuclear protein import. Cell *79*, 767-778.

Groves, M.R. Hanlon, N., Turowski, O., Hemmings, B.A., Barford, D. (1999). The structure of the protein phosphatase 2A PR65/A subunit reveals the conformation of its 15 tandemly repeated HEAT motifs. Cell *96*, 99-110.

Gruss, O.J., Carazo-Salas, R.E., Schatz, C.A., Guarguaglini, G., Kast, J., Wilm, M., Le Bot, N., Vernos, I., Karsenti, E., Mattaj, I.W. (2001). Ran induces spindle assembly by reversing the inhibitory effect of importin alpha on TPX2 activity. Cell *104*, 83-93.

Harel, A., Chan, R.C., Lachish-Zalait, A., Zimmerman, E., Elbaum, M., Forbes, D.J. (2003). Importin beta negatively regulates nuclear membrane fusion and nuclear pore complex assembly. Mol Biol Cell 14, 4387-4396.

Harel, A., and Forbes, D.J. (2004). Importin Beta: Conducting a much larger cellular symphony. Mol. Cell *16*, 319-330.

Hinshaw, J.E., Carragher, B.O., Milligan, R.A. (1992). Architecture and Design of the Nuclear Pore Complex. Cell *69,* 1133-1141.

Hutten, S., Walde, S., Spillner, C., Hauber, J., Kehlenbach, R.H. (2008). The nuclear pore component Nup358 promotes transportin-dependnet nuclear import. J Cell Sci *122*, 1100-1110.

Iijima, M., Suzuki, M., Tanabe, A., Nishimura, A., Yamda, M. (2006). Two motifs essential for nuclear import of the hnRNP A1 nucleocytoplasmic shuttling sequence M9 core. FEBS Lett *580*, 1365-1370.

Imasaki, T., Shimizu, T., Hashimoto, H., Hidaka, Y., Kose, S., Imamoto, N., Yamada, M., Sato, M. (2007). Structural basis for substrate recognition and dissociation by human transportin 1. Mol Cell *28*, 57-67.

Kalab, P., and Heald, R. (2008). The RanGTP gradient—a GPS for the mitotic spindle. J. Cell Sci. *121*, 1577–1586.

Kalab, P., Weis, K., and Heald, R. (2002). Visualization of a Ran-GTP gradient in interphase and mitotic *Xenopus* egg extracts. Science *295*, 2452–2456.

Lachish-Zalait, A., Lau, C.K., Fichtman, B., Zimmerman, E., Harel, A., Gaylord, M. R., Forbes, D. J., Elbaum, M. (2009). Transportin Mediates Nuclear Entry of DNA in Vertebrate Systems. Traffic *10,* 1414–1428.

Lau, C.K., Delmar, V.A., Chan, R.C., Phung, Q., Bernis, C., Fichtman, B., Rasala, B.A., Forbes, D.J. (2009). Transportin regulates major mitotic assembly events: From spindle to nuclear pore assembly. Mol. Bio. Cell *20,* 4043-4058.

Lee, B.J., Cansizoglu, A.E., Suel K.E., Louis, T.H., Zhang, Z., and Chook, Y.M. (2006). Rules for nuclear localization sequence recognition by karyopherin beta 2. Cell *126*, 543-558.

Levin, A., Hayouka, Z., Friedler, A., Loyter, A. (2010). Transportin 3 and importin α are required for effective nuclear import of HIV-1 integrase in virus-infected cells. Nucleus *1*, 422-431.

Lim, R.Y., Ullman, K.S., Fahrenkrog, B. (2008). Biology and biophysics of the nuclear pore complex and its components. Int Rev Cell Mol Biol *267*, 299-342.

Marelli, M., Dilworth, D.J., Wozniak, R.W., Aitchison, J.D. (2001). The dynamics of karyopherin-mediated nuclear transport. Biochem Cell Biol *79*, 603-612.

Maresca, T.J., and Heald, R. (2006). Methods for studying spindle assembly and chromosome condensation in Xenopus egg extracts. In Methods in Molcular Biology: Cell Biology and Signal Transduction. Liu X. Johne eds., (Totowa, NJ: Humana Press

Inc.) pp. 459-472.

Merle, E., Rose, R.C., LeRoux, L., Moroianu, J. (1999). Nuclear import of HPV11 L1 capsid protein is mediated by karyopherin alpha2beta1heterodimers. J Cell Biochem *74*, 628-637.

Mosammaparast, N., Pemberton, L.F. (2004). Karyopherins: from nuclear-transport mediators to nuclear-function regulators. Trends Cell Biol. *14*, 547-556.

Nachury, M.V., Maresca, T.J., Salmon, W.C., Waterman-Storer, C.M., Heald, R., and Weis, K. (2001). Importin beta is a mitotic target of the small GTPase Ran in spindle assembly. Cell *104*, 95-106.

Nelson, L.M., Rose, R.C., Moroianu, J. (2002). Nuclear import strategies of high risk HPV16 L1 major capsid protein. J Biol Chem *277*, 23959-23964.

Ohba, T., Nakamura, M., Nishitani, H., Nishimotot, T. (1999). Self-organization of microtubule asters in Xenopus egg extracts by GTP-bound Ran. Science 284, 1356-1358.

Orjalo, A.V., Arnaoutov, A., Shen, Z., Boyarchuk, Y., Zeitlin, S.G., Fontoura, B., Briggs, S., Dasso, M., and Forbes, D.J. (2006). The Nup107-160 nucleoporin complex is required for correct bipolar spindle assembly. Mol. Bio. Cell *17*, 3806-3818.

Paine, P.L., Moore, L.C., Horowitz, S.B. (1975). Nuclear envelope permeability. Nature *254*, 109-114.

Pollard, V.W., Malim, M.H. (1998). The HIV-1 Rev protein. Ann Rev Mircobiol *52*, 491-532.

Pollard, V.W., Michael, W.M., Nakielny, S., Siomi, M.C., Wang, F., and Dreyfuss, G. (1996). A novel receptor-mediated nuclear protein import pathway. Cell *86*, 985-994.

Rasala, B.A., Orjalo, A.V., Shen, Z., Briggs, S., Forbes, D.J. (2006). ELYS is a dual nucleoporin/kinetochore protein required for nuclear pore assembly and proper cell division. PNAS *103*, 17801-17806.

Reichelt, R., Holzenburg, A., Buhle Jr., E.L., Jarnik, M., Engel, A., Aebi., U. (1990). Correlation between structure and mass distribution of the nuclear pore complex and of distinct pore complex components. J. Cell Biol. *110,* 883–894.

Ren, M., Drivas, G., D'Eustachio, P. and Rush, M.G. (1993). Ran/TC4: a small nuclear GTP-binding protein that regulates DNA synthesis. J. Cell. Biol. **120**, 313–323

Rexach, M., Blobel, G. (1995). Protein import into nuclei: association and dissociation reactions involving transport substrate, transport factors, and nucleoporins. Cell *83*, 683-692.

Rout, M.P., Aitchison, J.D., Suprapto, A., Hjertaas, K., Zhao, Y., Chait, B.T. (2000). The yeast nuclear pore complex: composition, architecture, and transport mechanism. J. Cell Biol. *148*, 635–652.

Siomi, H., and Dreyfuss, G. (1995). A nuclear localization domain in the hnRNP A1 protein. J Cell Biol 129, 551–560.

Smith, A., Brownawell, A., Macara, I.G. (1998). Nuclear import of Ran is mediated by the transport factor NTF2. Curr Biol. *8*, 1403-1406.

Stade, K., Ford, C.S., Guthrie, C., Weis, K. (1997). Exportin1 (Crm1p) is an essential nuclear export factor. Cell *90*, 1041-1050.

Tsai, M.Y., Wang, S., Heidinger, J.M., Shumaker, D.K., Adam, S.A., Goldman, R.D., Zheng, Y. (2006). A mitotic lamin B matrix induced by RanGTP required for spindle assembly. Science *311*, 1887-1893.

Wilde, A., And Zheng, Y. (1999). Stimulation of microtubule aster formation and spindle assembly by the small GTPase Ran. Science 284, 1359-1362.

Xu, D., Farmer, A., Chook, Y.M. (2010). Recognition of nuclear targeting signals by Karyopherin-β proteins. Curr Opin Struct Biol *20*, 782-790.

Zhang, R., Mehla, R., Chauhan, A. (2010). Perturbation of Host Nuclear Membrane Component RanBP2 Impairs the Nuclear Import of Human Immunodeficiency Virus-1 Preintegration Complex. PLoS ONE *5,* e15620.